



Impact of land use on the hydraulic properties of the topsoil in a small French catchment

E. Gonzalez Sosa, Isabelle Braud, J. Dehotin, L. Lassabatère, Rafaël Angulo-Jaramillo, M. Lagouy, F. Branger, C. Jacqueminet, S. Kermadi, K. Michell

► To cite this version:

E. Gonzalez Sosa, Isabelle Braud, J. Dehotin, L. Lassabatère, Rafaël Angulo-Jaramillo, et al.. Impact of land use on the hydraulic properties of the topsoil in a small French catchment. *Hydrological Processes*, 2010, 24 (17), pp.2382 - 2399. 10.1002/hyp.7640 . hal-00507313

HAL Id: hal-00507313

<https://hal.science/hal-00507313>

Submitted on 30 Jul 2010

HAL is a multi-disciplinary open access archive for the deposit and dissemination of scientific research documents, whether they are published or not. The documents may come from teaching and research institutions in France or abroad, or from public or private research centers.

L'archive ouverte pluridisciplinaire **HAL**, est destinée au dépôt et à la diffusion de documents scientifiques de niveau recherche, publiés ou non, émanant des établissements d'enseignement et de recherche français ou étrangers, des laboratoires publics ou privés.

1

1 **Impact of land use on the hydraulic properties of the topsoil** 2 **in a small French catchment**

3

4 E. Gonzalez-Sosa,^{1,2} I. Braud,^{1*} J. Dehotin,¹ L. Lassabatère,³ R. Angulo-Jaramillo,^{4,5}
5 M. Lagouy¹, F. Branger¹, C. Jacqueminet⁶, S. Kermadi⁶, K. Michell⁶

7¹ Cemagref, UR HHLY, CP 220, 3bis Quai Chauveau, 69336 Lyon Cédex 9, France

8² DEFI-CIAQ, Université de Querétaro, CU Cerro de las Campanas. S/N. Centro. 6900
9 Queretaro, Qro., Mexico

10³ Laboratoire Central des Ponts et Chaussées, Division Eau et Environnement, Route de
11 Bouaye, 44381 Bouguenais Cedex, France.

12⁴ Université de Lyon, ENTPE, rue Maurice Audin, 69518 Vaulx-en-Velin, France

13⁵ LTHE, CNRS, BP 53, 38041 Grenoble Cedex 9, France

14⁶ Université de Lyon, UMR CNRS EVS, 18 rue de Chevreul, F-69 364 Lyon Cedex, France

15

16

17

18

19

20* Correspondance to: Isabelle Braud, Cemagref, UR HHLY, CP 220, 3bis Quai Chauveau,
21 69336 Lyon cedex 9, France

22 E-mail : Isabelle.Braud@cemagref.fr

23

24

25

26 *Hydrological Processes*, 2010, Vol 24, 2382-2399, DOI: 10.1002/hyp.7640

1

1Abstract

2The hydraulic properties of the topsoil control the partition of rainfall into infiltration and
3runoff at the soil surface. They must be characterized for distributed hydrological modelling.
4This study presents the results of a field campaign documenting topsoil hydraulic properties
5in a small French suburban catchment (7 km²) located near Lyon, France. Two types of
6infiltration tests were performed: single ring infiltration tests under positive head and tension
7disk infiltration using a mini-disk. Both categories were processed using the BEST –*Beerkan*
8Estimation of Soil Transfer parameters- method to derive parameters describing the retention
9and hydraulic conductivity curves. Dry bulk density and particle size data were also sampled.
10Almost all the topsoils were found to belong to the sandy loam soil class. No significant
11differences in hydraulic properties were found in terms of pedologic units, but the results
12showed a high impact of land use on these properties. The lowest dry bulk density values
13were obtained in forested soils with the highest organic matter content. Permanent pasture
14soils showed intermediate values, whereas the highest values were encountered in cultivated
15lands. For saturated hydraulic conductivity, the highest values were found in broad leaved
16forests and small woods. The complementary use of tension disk and positive head infiltration
17tests highlighted a sharp increase of hydraulic conductivity between near saturation and
18saturated conditions, attributed to macroporosity effect. The ratio of median saturated
19hydraulic conductivity to median hydraulic conductivity at a pressure of -20 mm of water,
20was about 50. The study suggests that soil texture, such as used in most pedo-transfer
21functions, might not be sufficient to properly map the variability of soil hydraulic properties.
22Land use information should be considered in the parameterizations of topsoil within
23hydrological models to better represent *in situ* conditions, as illustrated in the paper.

24

1

1Keywords: soil hydraulic properties, infiltration tests, BEST method, land use impact,
2hydraulic properties mapping

1

1INTRODUCTION AND CONTEXT

2

3Soil surface thermal and hydraulic properties control heat and water exchange at the soil
4vegetation atmosphere interface through their impact on infiltration and the surface energy
5balance. Therefore, they play a central role in the correct understanding and modelling of
6water balance, surface processes, evapotranspiration, groundwater recharge, erosion or
7pollutant transport. Human activities such as agricultural practices (ploughing, sowing),
8changes in land use related to urbanisation, industrial activity, deforestation or reforestation of
9abandoned agricultural land can significantly affect topsoil and first layers hydraulic
10properties. The accurate representation of soil hydraulic properties within hydrological
11models is therefore necessary to reliably represent the water balance and hydrological
12responses. In many hydrological models, soil hydraulic properties are determined based on
13pedo-transfer functions. These functions relate easily accessible soil properties such as soil
14texture (e.g. Clapp and Hornberger, 1978; Cosby *et al.*, 1984) or soil texture, organic matter
15content and dry bulk density (e.g. Rawls and Brackensiek, 1985; Verecken *et al.*, 1989;
16Wösten, 1997) to soil hydraulic properties (retention and hydraulic conductivity curves).
17Existing pedo-transfer functions have been in general calibrated on limited soil samples and
18are often region specific. As an illustration, the pedotranfer functions of Cosby *et al.*, (1984)
19and Rawls and Brackensiek (1985) were calibrated on US soils. Verecken *et al.* (1989) used
20soil samples from Belgium, and Wösten (1997) the HYPRES European soil data base
21(Wösten *et al.*, 1999). Different conclusions have been reached about the use of pedotransfer
22functions in hydrological models. Some studies have concluded that existing pedo-transfer
23functions are adequate (e.g. Islam *et al.*, 2006) whereas other authors question their usefulness
24for a correct assessment of hydrological water balances (e.g. Sobieraj *et al.*, 2001; Gutman
25and Small, 2005). Wösten *et al.* (2001) underline the usefulness of pedotransfer functions but

1discourage their use for soils that are outside their range of applications, while calling for the
2collection of large data sets to document soil hydraulic properties worldwide.

3The present study is based on these recommendations and contributes to the documentation of
4soil hydraulic properties in a small French suburban catchment. Suburban catchments
5generally experience a large and quick land-use change, such as an increase of impervious
6areas, but also sometimes, desertion of farming lands that turn into fallow lands, and finally
7into sporadic deciduous forests. Rivers and runoff are also affected through straightening of
8natural water courses and runoff concentration into pipes for instance. A higher proportion of
9built infrastructures has a significant impact on hydrologic and ecosystem functions and often
10result in excess runoff, lower groundwater recharge and pollution (e.g., Bras and Perkins,
111975; Desbordes, 1989; Chocat *et al.*, 2001; Booth *et al.*, 2002; Randhir, 2003; Matteo *et al.*,
122006; Marsalek *et al.*, 2007). The vulnerability of these areas to floods, droughts and water
13quality problems is therefore increased.

14The Yzeron catchment (150 km²) is located to the south-west of Lyon city (Figure 1). This
15catchment is representative of many suburban catchments. Since the fifties, it has experienced
16rapid changes of land use, due to the vicinity of Lyon city. Two different trends can be
17observed since the middle of the 20th century. The first one is an increase of the catchment
18urbanisation, with a full urbanised area in the downstream part. The second trend is a decrease
19of cultivated land explained by the urbanisation, but also by an increase of the forested areas
20in relation with the decline of agricultural activities (Gnouma, 2006). In recent years, several
21problems have been identified: an increase in the frequency of flooding (Radojevic, 2002),
22increased pollution problems (Lafont *et al.*, 2006), and increased erosion of the river banks
23associated with adverse effects on water quality (Schmitt *et al.*, 2008). The water responsible
24for these flooding events comes mainly from the rural part of the catchment, but its effect can
25be enhanced by fast contributions from urbanised zones having short runoff lag time

1

1(Radojevic, 2002). These disorders must be reduced to comply with the requirements of the
2water framework directive. It is therefore important to better quantify the impact of land use
3changes on the hydrological regime of this catchment. For this purpose, a distributed
4hydrological model of the catchment is being developed, that takes into account both the rural
5and the urbanised areas. Given the importance of rural areas on the Yzeron regime, it was
6necessary to acquire improved knowledge on the soil hydraulic properties within the
7catchment and propose rules for their specification in the elementary meshes of the distributed
8hydrological model (from a few hectares to a few km²). This task is of course challenging,
9because it is not possible to measure soil hydraulic properties everywhere and we wanted to
10propose alternative solutions to the use of pedo-transfer functions only, by introducing *in situ*
11observations in the mapping process.

12The objectives of the study were the following: (i) to document the spatial variability of soil
13hydraulic properties (including both the retention and hydraulic conductivity curves) within
14the catchment using relevant *in situ* measurements and an adequate sampling strategy; (ii) to
15analyse the links between the spatial variability of hydraulic properties and pedology and land
16use; (iii) to use these measurements to derive rules for the mapping of soil hydraulic
17properties as required in distributed hydrological modelling.

18

19MATERIALS AND METHODS

20Catchment description

21The Yzeron catchment is located south-west of Lyon city in the “Mont du Lyonnais” area
22(Figure 1). The topography ranges from a maximum of 917 m above sea level in the western
23part to a minimum of 162 m at the outlet. The highest slopes are encountered in the western
24part of the catchment and along the river network and the lowest slopes are located in the

1eastern part (Figure 1). The geology is composed mainly of gneiss and granite. The average
2annual rainfall is 800 mm and the average annual minimum and maximum temperatures are
36.8 °C and 15.8 °C, respectively (Gnouma, 2006). The catchment forms part of a long term
4observatory called Observatoire de Terrain en Hydrologie Urbaine (OTHU, 2010), dedicated
5to the study of the impact of urbanisation on hydrology. In this framework, two sub-
6catchments have been monitored since 1997. The first one, the Mercier catchment (7 km²) is
7considered as a natural catchment and is covered mainly with forests and crops. The second
8one, the Chaudanne catchment (2.5 km²) is mainly covered with crops and urbanised areas
9(Figure 1). The Mercier catchment shows a large spatial variability of soils, with the presence
10of 8 soil pedological units over a total of 22 present within the whole Yzeron catchment,
11according to the Sol Info Rhône Alpes pedology map (SIRA, 2010). The Mercier catchment
12soils are also representative of the rural area of the Chaudanne catchment. The study
13presented here is therefore focused on the Mercier catchment. In this basin, the elevation
14ranges from 400 m and 800 m with a marked topography and slopes commonly higher than
1510%. The land use is dominated by forest, pasture and crops, although a significant part of the
16catchment is affected by human activity with the existence of small villages and a quite dense
17road network.

18

19*Sampling strategy*

20The sites were selected to include the maximum combinations of factors that can influence
21soil hydraulic properties such as pedology and land use. For this purpose, we used the
22pedology map, provided by Sol Info Rhône Alpes at scale 1/250000 (Figure 2, SIRA, 2010)
23and the 2000 Corine Land Cover map provided by the Service de l'Observation et des
24Statistiques (SOeS, 2010). The distribution from the land use map showed that the forest area
25(mountain) represents about 33%, pasture 32% and complex cultivation pattern accounts for

1

about 30% of the total basin area. Urbanised surface is less than 6% of the total surface. Regarding soil classes, soil 102 (loamy sand and clayey sand – see Table I) covers more than 350% of the basin area. From this analysis, nine soil classes and six land uses from the Corine map were retained that accounted for most of the total area and a first selection of sites was performed in order to sample the maximum of land use/pedology combinations (17 over a total of 38 covering 90% of the catchment surface). Sites accessibility was also taken into account in the final selection. A field survey refined the selection and the land use description, especially for crops where the Corine land cover map was not detailed. Finally 20 locations were retained and sampled (Figure 2). Their distribution in terms of pedology (Soil Cartographic Units –SCU-) and land use, as retrieved from the field, is shown in Table I. The measured points within the sites were located at least 10 m from the fields edges. With regard to topography, most of the sites were located on slopes, very few in flat zones. At the 320 locations, samples were collected in order to characterize the soil texture and the dry bulk density. Infiltration tests using single ring and mini-disk infiltrometers were performed. The field survey was restricted to the topsoil layer. The location of each infiltration test was measured using a GPS (3 m in x and y). The experimental protocols are described below.

17

18 *Soil texture and dry bulk density measurements*

19 Twenty-eight topsoil samples of 250-300 g were collected using augers and were analysed to 20 derive the soil particle size distribution function. Five classes were considered (clay, fine silt, 21 coarse silt, fine sand, coarse sand) corresponding to the following fractions (<2 , 2-20, 20-50, 22 250-200, 200-2000 μm) and were determined according to the French standard (NF X 31-107 23 norm), which involves sieving for the fractions $>50 \mu\text{m}$ and sedimentation below 50 μm . 24 Organic matter content was also determined using the NF ISO 10694 standard. All the 25 analyses were done at the INRA soil laboratory in Arras .

To characterize the topsoil A horizon, the dry bulk density was measured using samples collected in the 0-2.5 cm depth and 0-5 cm depth layers. These samples were collected following the ISO NF X31-501 standard. The dry bulk density, ρ_d , allows the derivation of porosity once assumed a certain value for the particle density, ρ_s . In this study we used the commonly used value of $\rho_s = 2650 \text{ kg m}^{-3}$ and the porosity, ε , was calculated as:

$$\varepsilon = 1 - \frac{\rho_d}{\rho_s} \quad (1)$$

Infiltration tests

The field campaign was conducted from October 6 to October 10 2008 by a team of five persons. At each of the twenty selected locations, infiltration tests were performed using two techniques: Mini Disk Infiltrometer (MDI) (in general two replicates per location) and single ring (SR) or *Beerkan* method (Braud *et al.*, 2005) (three replicates per location). Their distribution with respect to pedological cartographic units and land uses is shown in Table I. Braud *et al.* (2005) proposed an experimental protocol for the single ring infiltration tests, with cylinders of 5-15 cm in diameter. According to this protocol, about 8-15 equal volumes of water must be poured successively into the cylinders. The infiltration times of these water volumes are measured. In our study, the cylinders used for the SR tests were 400 mm in diameter and 225 mm in height. They were much larger than recommended by Braud *et al.* (2005). The reason of this choice is the wish to average the soil spatial heterogeneity by sampling a larger surface, in order to obtain measures representative of the fields. As a consequence, the infiltration protocol had to be modified as compared to Braud *et al.* (2005). Before each SR test, the litter and vegetation leaves were removed, as in Bodhinayake and Si (2004). If necessary, the vegetation was cut but roots were left in place. The cylinders were inserted 2-5 cm deep into the soil, in order to ensure water tightness and avoid leaks, without perturbing too much the 3-D water flow. In all cases 12 L of fresh (15-18 °C) water were

1

1 poured within a plastic sheet, sealed to the cylinder, to minimize the disturbances in topsoil
2 that frequently occur when water is added directly. The plastic sheet was then removed and
3 the chronometer was started. The initial height was measured using a ruler. Then the
4 infiltration height as a function of elapsed time was followed by reading the ruler. During the
5 first minutes, small time intervals of a few seconds were used and the time interval was
6 increased after 3 or 5 minutes (Herman *et al.* 2003). The operation was terminated when all
7 the water had infiltrated the soil. Two soil samples were also collected for measurement of
8 the initial and final gravimetric water contents (g water per g solids). For the final water
9 content sampling, small cylinders of 43 mm in diameter and 28 mm in height were used.
10 These samples enable us to obtain additional measurements of the dry bulk density.
11 For the MDI infiltration tests, we used the tension Mini-disk Infiltrometer of 135 ml in
12 volume water capacity and 22.5 mm in radius (Decagon Devices Inc., Pullman, WA). The
13 detritus and dead leaves were also removed before the tests started. A small layer of soil
14 (Horizon O < 5 cm) of less than 2 cm was also removed. It was required in order to carry out
15 the tests on horizontal surfaces and ensure the stability of the apparatus and a good contact
16 between the infiltrometer membrane and the soil. For this we used a thin layer (< 1mm) of
17 fine sand. The surface pressure was set to -20 mm for all the MDI infiltration tests.

18

19 *Derivation of retention and hydraulic conductivity curves parameters using the BEST method*

20 The infiltration tests were used to determine the retention curve $h(\theta)$, relating the soil water
21 pressure h (m) to the soil volumetric water content θ ($\text{m}^3 \text{m}^{-3}$) and the hydraulic conductivity
22 curve $K(\theta)$ relating the soil hydraulic conductivity K (m s^{-1}) to the soil water content. The
23 retention curve was modeled using the van Genuchten (1980) approach:

1

$$\frac{\theta}{\theta_s} = \left\{ 1 + \left(\frac{h}{h_{VG}} \right)^n \right\}^{-m} \quad (2)$$

$$\text{with } n = \frac{k}{1-m} \quad (3)$$

where θ_s is the saturated water content ($\text{m}^3 \text{ m}^{-3}$), h_{VG} (m) is a normalization parameter for the water pressure, m and n are shape parameters (-) and k is an integer which can be chosen to be (Mualem, 1976) or 2 (Burdine, 1953). A value of $k=2$ was used in the following. A value of $k=1$ could have been used either as Haverkamp *et al.* (2005) provide relationships between the various formulations. Eq. (2) assumes that the residual water content at large pressure is zero.

The hydraulic conductivity curve was modeled using the Brooks and Corey (1964) model:

$$K(\theta) = K_s \left(\frac{\theta}{\theta_s} \right)^\eta \quad (4)$$

where K_s (m s^{-1}) is the saturated hydraulic conductivity and η is a shape parameter (-) related to m and n by:

$$\eta = \frac{2}{mn} + 2 + p \quad (5)$$

where p is a tortuosity parameter equal to 0 (Childs and Collis-George, 1950), 0.5 (Mualem, 1976) or 1 for the Burdine (1953) model. A value of 1 was used in this study to be consistent with the choice of the Burdine (1953) model for the retention curve in Eq. (3).

At each location, the values of the parameters of the retention and hydraulic conductivity curves as described by Eqs. (2) and (4), namely the shape parameters m , n and η and the structure parameters θ_s , h_{VG} and K_s were calculated. It was done using the BEST (*Beerkan Estimation of Soil Transfer parameters*) method proposed by Lassabatère *et al.* (2006). The first step of the BEST method corresponds to the estimation of the shape parameters m , n and

1

1 η from the soil particle size distribution data. Details can be found in Lassabatère *et al.* (2006)

2 and are not reported here.

3 The second step is the optimisation of the infiltration tests in order to derive the structural
4 parameters θ_s , h_{VG} and K_s . In this study, the saturated water content, θ_s , was determined from
5 field final water content and dry bulk density and therefore only h_{VG} and K_s were derived from
6 the optimisation of the infiltration tests. Two equations were used for this purpose.

7 For short to medium time steps, the BEST method uses an analytical approximation of the full
8 3D infiltration, $I_{3D}(t)$ (m), equation proposed by Haverkamp *et al.* (1994) for the interpretation
9 of infiltration tests:

$$10 \quad I_{3D}(t) = S\sqrt{t} + \left[\frac{\phi S^2}{R(\theta_0 - \theta_i)} + K_i + \frac{2 - \beta}{3}(K_0 - K_i) \right] t \quad (6)$$

11 where S is the sorptivity ($\text{m s}^{-1/2}$); R is the radius of the infiltrometer (m), θ_i is the initial
12 water content and θ_0 is the final water content, K_i is the initial hydraulic conductivity (m s^{-1})
13 and K_0 (m s^{-1}) is the final one. $K_0 = K(h_0)$, where h_0 (m) is the water pressure at the soil
14 surface (positive for single ring infiltration tests and negative for mini-disk infiltration tests).
15 For the parameters β and ϕ , we used the value of $\phi=0.75$ and $\beta=0.6$, shown to apply for most
16 soils when $\theta_i < 0.25 \theta_s$ (Smettem *et al.*, 1994; Haverkamp *et al.*, 1994). The sorptivity
17 $S(\theta_i, \theta_0)$ is a function of initial and final water content but notation $S = S(\theta_i, \theta_0)$ will be used
18 for the sake of simplicity.

19 The approximation provided by Eq.(6) is valid only for times t_i lower than a maximum value
20 given in Lassabatère *et al.* (2006):

$$21 \quad t_{\max} = \frac{1}{4(1 - B)^2} t_{\text{grav}} \quad (7)$$

$$22 \text{ where } B = \frac{K_i}{K_0} + \frac{2 - \beta}{3} \left(1 - \frac{K_i}{K_0} \right) = \left(\frac{\theta_i}{\theta_0} \right)^\eta + \frac{2 - \beta}{3} \left(1 - \left(\frac{\theta_i}{\theta_0} \right)^\eta \right) \quad (8)$$

1

$$1 \text{ and } t_{grav} = \left(\frac{S}{K_0} \right)^2 \quad (9)$$

2 t_{grav} is the gravity time which corresponds to the time at which gravity begins to dominate the
3 flow process (Philip, 1969).

4 For long time steps, Haverkamp *et al.* (1994) showed that the asymptotic infiltration can be
5 written (subscript _{3D} is omitted in the following for simplicity):

$$6 \quad I_{\infty} = \left[K_0 + \frac{\phi S^2}{R(\theta_0 - \theta_i)} \right] t + \frac{S^2}{2(K_0 - K_i)(1 - \beta)} \ln \left(\frac{1}{\beta} \right) \quad (10)$$

7 which corresponds to a linear variation with time. For long time steps, the infiltration flux is a
8 constant given by the slope of the curve $I(t)$ as defined by Eq. (10):

$$9 \quad q_{\infty} = K_0 + \frac{\phi S^2}{R(\theta_0 - \theta_i)} = K_0 + AS^2 \quad (11)$$

$$10 \text{ with } A = \frac{\phi}{R(\theta_0 - \theta_i)} \quad (12)$$

11 Data for large time steps are used to fit Eq. (10) using a simple regression analysis and derive
12 the q_{∞} estimate. For short times steps, we used the method proposed by Lassabatère *et al.*
13 (2006) to optimize the sorptivity. The reader can refer to this paper for more details.

14 Note that, up to this step, the method can be applied both for infiltration test under suction or
15 with a positive pressure head. Therefore it can be used for the interpretation of both the mini-
16 disk and single ring infiltration tests.

17 On the other hand, the estimation of the normalization parameter h_{VG} can only be performed
18 from the SR infiltration (Braud *et al.*, 2005) using:

$$19 \quad h_{VG} = - \frac{S^2}{c_{p-VG}(\theta_s - \theta_i)K_s \left[1 - \left(\frac{\theta_i}{\theta_s} \right)^{\eta} \right]} \quad (13)$$

1

where c_{p_VG} is a texture dependent factor, the expression of which is given by Haverkamp *et al.* (1998):

$$c_{p_VG} = \Gamma\left(1 + \frac{1}{n}\right) \left\{ \frac{\Gamma\left(m\eta - \frac{1}{n}\right)}{\Gamma(m\eta)} + \frac{\Gamma\left(m\eta + m - \frac{1}{n}\right)}{\Gamma(m\eta + m)} \right\} \quad (14)$$

where Γ is the classical incomplete Gamma function.

Up to now, only positive head infiltration tests have been analysed using the BEST method (de Souza *et al.*, 2008; Mubarak *et al.*, 2009; Xu *et al.*, 2009). The only exception is the case study by Scalenghe and Ferraris (2009) that also analysed tension-disk infiltration tests with the method. To our knowledge, it is also the first time that the method is used on terrain with a significant slope and using cylinders with so large diameters.

10

11 *Statistical analysis of data*

The data were analysed using statistical tests from the R packages (R Development Core Team, 2004). Kolmogorov-Smirnov or χ^2 tests were performed to test the hypothesis of normal distribution of the data. When appropriate, i.e. independent normal distribution for residuals, along with equality in variances, Student t-tests were performed to study the degree of significance of differences in averages amongst different factors (pedology and land use classes). Otherwise, non parametrical tests (Kruskal-Wallis / Wilcoxon tests) were performed. Results are presented in terms of the critical probability p that quantifies the risk to be wrong when rejecting the null hypothesis (no effect and no difference). If $p < 0.05$ (respectively < 0.10), then the hypotheses of equality of mean/variance/distribution is rejected at the 5% (respectively 10%) level and the difference amongst classes can be considered as significant at this level.

1The replicates were considered as independent samples in the statistical analysis. Except three
2points, the sampled points within the same field were distant from more than 20 m. The
3distance between fields was more than 50-100 m. In the recent synthesis proposed by van der
4Keur and Iversen (2009), soil porosity is reported to have a spatial correlation ranging from 0
5to about 75 m from three different studies. Saturated hydraulic conductivity spatial correlation
6is reported to range between 0 and about 40 m in six studies. These figures and the fact that
7most of the points were collected in different fields, even at the same site, justify our
8independence hypothesis of the measurement points.

9RESULTS

10In this section, we discuss the results in terms of soil texture, soil porosity, fitting of the
11infiltration tests. Then, results of the single ring infiltration tests, and of mini-disk infiltration
12tests, are discussed. Finally, results are summarised in terms of retention and hydraulic
13conductivity curves. A mapping of the topsoil surface properties over the Mercier catchment
14is also proposed.

15Soil texture

16The soil particle size distribution was measured using 28 samples of the topsoil. Figure 3a
17presents the results for clay, fine and coarse silt, fine and coarse sand. Table II summarizes
18these results as well as those of the shape parameters n and η of the retention and hydraulic
19conductivity curves. Figure 4 presents all the sample points in the USDA textural triangle. It
20shows that all the topsoil A horizons belong to the sandy loam soil class except one loam, one
21silty clay loam and two loamy sands. However, the variability of texture within the sandy
22loam class is quite large. The soils have generally a coarse texture, with an average sand
23content of 67.5%. The coefficient of variation of the sand fractions is about 20%. The clay
24content is 13% on average, with a lower coefficient of variation (14%). The silt content is

about 20% on average, with the largest coefficient of variation (30%). The χ^2 goodness of fit test showed that the Gaussian distribution was acceptable for all the fractions ($p > 0.10$). The Kruskal-Wallis test showed no significant differences in distribution in terms of Soil Cartographic Unit (SCU) for all the fractions except the fine sand fraction at the 5% level ($p = 0.02$), the coarse silt fraction ($p = 0.09$), and the coarse sand fraction ($p = 0.094$) at the 10% level.

The organic matter content shows a high variability with a coefficient of variation of about 850% ranging from 2 to 13%, with the highest content in forest soils and pasture. The Gaussian distribution is also acceptable for organic matter ($p = 0.57$). The Kruskal-Wallis test showed significant differences at the 10% level in terms of land use ($p = 0.08$) but not in terms of SCU ($p = 0.17$).

Table II also provides the shape parameters of the retention and hydraulic conductivity curves n and η . The n parameter should be larger than two so that m derived from Eq.(3) is positive. The average value of n (2.17) is therefore quite low and its variability is small (CV of about 152%). The η parameter has a mean value of 15.2 and a higher coefficient of variation (20%). The Gaussian distribution was found acceptable for n at the 5% level ($p = 0.07$), and η at the 10% level ($p = 0.12$). The n and η parameters have small coefficient of variations and the average value can be considered as representative of the catchment. However, this hypothesis must be verified using the distributed hydrological model. These parameters control the decay of the retention and hydraulic conductivity curves when the soil dries out, through a power function. And some authors have reported a high sensitivity of water balance components to small variations of n (e.g. Braud, 1998; Boulet *et al.*, 1999).

Dry bulk density and porosity

The dry bulk density estimated using the 0-2.5 cm height and the 0-5 cm height cylinders are compared in Figure 5a. The correlation is good, $R^2 = 0.85$ ($p < 10^{-6}$, 19 samples), with values of

1

the dry bulk density in general lower when using the smaller cylinders. This result is not surprising as the 0-2.5 cm height samples consist almost exclusively of topsoil which contains more organic matter and vegetation residues. The average dry bulk density of all the samples was 1078 kg m^{-3} (± 318). This value is quite low. Soil 704, classified as loamy sand to clayey sand presents the highest density of 1330 kg m^{-3} (± 281). In contrast soil 1031 (loamy sand from tuffs) shows the lowest average of 709 kg m^{-3} (± 135).

The statistics of the 0-5 cm height values with respect to land use classes are presented in Table III, as well as the statistics of organic matter and porosity (see also Figure 3b). As expected, the highest organic matter contents are observed in permanent pasture and forest soils whereas the lowest values are encountered in the cultivated fields. Points with the highest organic matter content are associated with the lowest dry bulk density and highest porosity. This is illustrated in Figure 5b which shows the correlation between dry bulk density and organic matter content. The correlation is significant with $R^2=0.54$ ($p = 10^{-5}$, 27 samples).

14

The statistics of organic matter and dry bulk density with respect to pedologic units (SCU) are not shown in Table III as the Kruskal-Wallis test indicated that differences amongst classes were not significant at the 10% level ($p=0.18$) when soil 1031, exhibiting the lowest values, was excluded. The differences in terms of land use were significant. The Wilcoxon rank sum test (or Mann-Witney test) was performed for all the combinations of two land use groups. It allowed the proposition of three main classes of dry bulk density by gathering the classes where the p -value was higher than 0.1. One class could be identified easily corresponding to forest soils (broad leaved and coniferous forests) with the lowest dry bulk density and highest organic matter content (class DB1). For the two other classes, it was not so easy to distinguish between land uses, especially for land use 4 (bare soil after ploughing). Based on the largest p values, we defined the two other classes as follows: permanent pasture, clearing and small

1 woods for class DB2, with intermediate dry bulk density; and cultivated pasture, crops and
2 orchards for class DB3 with the highest dry bulk density. The statistical properties of the
3 variables with respect to these new classes are presented in Table IV. We verified *a posteriori*
4 that the classification was relevant, as the p value amongst any pair of classes was lower than
5 10^{-6} . A cluster analysis of the points, described using dry bulk density and organic matter
6 content, led to the same three main classes as the method presented above. It strengthens the
7 conclusion that land use has a strong impact on the topsoil dry bulk density. This can be
8 explained by agricultural practices and machines that induce a higher dry bulk density
9 corresponding to a soil compaction.

10 The same classes are obtained for porosity, as the latter is a decreasing function of the dry bulk
11 density.

12 We mentioned before that the final water content θ_0 was assumed to be equal to the saturated
13 water content. To assess the consistency of this hypothesis, we calculated the ratio θ_0/ε . Three
14 points had values higher than 1 and the final water content was thus set to the porosity. The
15 range of the values was large: [0.35-1]. Values lower than 0.4 were associated to forest or
16 small woods soils with a high organic matter content and a high porosity. The hydrophobic
17 effect of organic matter could also influence these results. The average of the ratio was $0.7 \pm$
18 0.18 (57 points), a value much lower than the values commonly reported in the literature $0.8-1$
19 (Rogowski, 1971). Table IV shows the values of this ratio per dry bulk density classes (DB1,
20 DB2 and DB3). It shows a large range of values for the three classes with a range of [0.3-1.0]
21 in all cases. Contrary to what happens for dry bulk density and porosity, the differences
22 amongst the three classes are not significant for this ratio with values of the Wilcoxon rank
23 sum test p -values larger than 0.65.

1

1

2Fitting of single ring and mini-disk infiltration tests

3Due to the experimental protocol (small oscillations of the water surface just after removing
4the plastic sheet), there were some uncertainties on the initial level within the cylinder.
5Furthermore, due to the terrain slope (from zero to about 10%), the initial value was not
6always equal to the nominal value corresponding to the water volume divided by the cylinder
7surface, i.e. 95.5 mm. The initial level was thus adjusted manually to ensure data consistency.
8In order to assess *a posteriori* the reliability of the fitted parameters for the two methods, we
9calculated the gravitational time given by Eq. (9). For 76% of the SR infiltration test and 65%
10of the MDI tests, the total infiltration time was larger than the gravitational time. Thus the
11asymptotic regime could be assessed with a good accuracy for these tests and all the data were
12processed using both Eq. (6) and Eq. (10). On the other hand, the short time infiltration Eq.
13(6) could be valid for only a very few points, leading to less robust estimation of sorptivity.
14This is illustrated on Figure 6a where only the 6 first data points fit the short time model and
15the other points fit the asymptotic equation. In this case, the influence of capillary force was
16very short and the gravitational time was reached after about 100 s. In this case, the sorptivity
17was estimated with only a small number of points which can be detrimental to the robustness
18of the optimization, but is theoretically adequate. When the maximum infiltration time was
19lower than the gravitational time, the short time model of Eq. (6) was valid for the whole
20infiltration test duration. In this case, the estimated sorptivity was numerically robust, whereas
21the estimation of the asymptotic regime was less easy. This is illustrated in Figure 6b where
22the slope of the long time infiltration curve (Eq.(10)) is parallel to the asymptotic infiltration
23equation (dashed line) and the data fit the short time model up to the end. It shows that the
24gravitational time was not yet reached. For these infiltration tests, the effect of the terrain
25slope on the results was thus minimum and the estimation of sorptivity was robust (Chen and

1

1Young, 2006). Figure 6 illustrates the SR data but the same kind of results was obtained for
2the mini-disk infiltration data.

3For the SR infiltration tests, the average gravitational time was $6 \text{ min} \pm 14 \text{ min}$ and, for the
4MDI infiltration tests, the average was $60 \text{ min} \pm 138 \text{ min}$. It can be compared to the
5infiltration test duration which was $10 \text{ min} \pm 19 \text{ min}$ for SR and $33 \text{ min} \pm 35 \text{ min}$ for the MDI
6infiltration tests. Capillary effects were thus very short for the positive head infiltration tests,
7whereas they lasted much longer for tension-disk infiltration. In both cases however, the use
8of the BEST method for optimization allowed to exploit at best the available data both before
9and after the gravitational time was reached.

10

11Single ring infiltration tests

12Table V shows the results of the infiltrated depth and maximum infiltration time. The values
13show that the infiltrated depth was close to the nominal value (volume of water / cylinder
14surface = 95.5 mm) with a median of 90 mm. Only four points did not work very well and had
15a much smaller infiltration depth. The slope of the terrain over which the cylinders were
16installed was responsible for this difference between the real and nominal infiltrated depths.
17In terms of maximum infiltration time, the range was from a few seconds (15 s) to 114 min
18for the longest test, with an average value of about 10 min and a median of about 3 min. Thus
19half of the infiltration tests took place in less than 3 min, which was very rapid and allowed to
20minimize the possible effect of slope on the infiltration. The high infiltration rates can also be
21related with preferential flow, which is not sensitive to slope effect. Only three tests had
22duration larger than 45 min, and two of them were located on flat areas.

23As in de Condappa (2005), we introduce the ratio

$$24 \quad L = I_{\max} / t_{\max} \quad (15)$$

1 where I_{max} (mm) is the maximum infiltrated depth and t_{max} (s) is the time to infiltrate this
2 quantity. As all the infiltration tests had about the same maximum infiltrated quantity, this
3 ratio could be used to rank the infiltration tests in terms of “infiltration capacity”. The
4 corresponding statistics are also provided in Table V. The average value is about 56 mm min^{-1}
5 and the median 27 mm min^{-1} . These values show very high infiltration capacity for the
6 catchment.

7 The statistics of estimated sorptivity and saturated hydraulic conductivity are provided in
8 Table III categorized in terms of land use. As for dry bulk density, differences in K_s were not
9 found significant in terms of pedology, with a value of the Kruskal-Wallis test of $p=0.14$.
10 Significant differences were found in terms of land use. Three main classes could be
11 identified (Figure 7). One class, class KS1, could be distinguished clearly. It was composed of
12 land use 6 and 9 (broad leaved forest and small woods) with the highest saturated hydraulic
13 conductivity and sorptivity (Table VI). The other land use classes could not be distinguished
14 so easily and were defined based on the largest p values. Class KS2 includes land uses 2, 4,
15 and 7 (cultivated pasture, bare soil after ploughing and clearing) with the lowest saturated
16 hydraulic conductivity and sorptivity (Table VI). Finally class KS3 contains the other land
17 uses (1, 3, 5, 8), namely permanent pasture, crops – wheat stubble and orchards-, and
18 coniferous forest, with intermediate saturated hydraulic conductivity (Table VI). We verified
19 *a posteriori* that the differences in distribution remained significant for both variables with the
20 new classes with p -values of the Wilcoxon rank sum test lower than 0.006. Table VI also
21 provides the statistics of the h_{VG} parameter. No significant differences amongst land use
22 classes was found for h_{VG} with p -value of the Wilcoxon-test larger than 0.2. The value for h_{VG}
23 is then considered as the same for all the KS and DB classes.

24 The classes in terms of saturated hydraulic conductivity are different from the classes
25 identified for dry bulk density. In particular, coniferous forest and broad leaved forests were

1

1 in the same group for dry bulk density. It is not the case for saturated hydraulic conductivity,
2 which shows that organic matter content and dry bulk density are not the only factors
3 influencing K_s .

4

5 *Tension-disk infiltration tests and comparison between the two methods*

6 At first, data analysis was conducted using traditional methods as described in Smiles and
7 Knight (1976) or Vandervaere et al. (2000a). These methods fit only the short to medium time
8 infiltration model of Eq. (6) and only a small amount of the data could be used. The
9 estimation was not robust and mostly produced negative hydraulic conductivity values. This
10 was not surprising, given the small cylinder radius and short transient stage of infiltration.
11 Indeed, Vandervaere et al. (2000b) showed that, in these experimental conditions, their ST
12 (single test) method was not recommended. The results are therefore not discussed below. We
13 saw that the BEST method uses the whole infiltration test data, including the asymptotic
14 regime. It allowed the derivation of reliable sorptivity and hydraulic conductivity estimates
15 for 39/43 MDI infiltration tests. The rejected tests were in general conducted in forest or
16 permanent pasture, where the impact of macropores might have been large and where the size
17 of the apparatus (45 mm in diameter) did not allow aggregation of the soil heterogeneity.
18 Table VI presents the statistics of the parameters derived from the mini-disk infiltrometer for
19 the three classes identified for saturated hydraulic conditions. As expected, sorptivity and
20 hydraulic conductivity were larger for the SR than for the MDI infiltration tests. The
21 Wilcoxon rank sum tests showed that differences in distribution amongst KS classes was not
22 significant for sorptivity and only significant for class KS3 for hydraulic conductivity. The
23 impact of land use change on hydraulic properties was thus most pronounced at saturation.
24 Table VI also provides the ratio between K_s and $K(-20 \text{ mm})$. The most striking result was the
25 sharp increase of hydraulic conductivity from near saturation (-20 mm of water pressure) to

1

1saturation with a ratio between the averages larger than 500, and a ratio between the median
2of 46.

3

4Retention and hydraulic conductivity curves

5All the results presented in the paper can be summarized by showing the retention and
6hydraulic conductivity curves typical for the combination of the DB and KS land use classes.
7They are shown in Figure 8 where average values of shape parameters from Table II, average
8values of saturated water content (calculated as average porosity times average θ_s/ε ratio)
9from Table IV and averages values of h_{VG} , K_s and $K(-20\text{ mm})$ in Table VI were used. The three
10retention curves differ mainly in saturated water content, as the same values of h_{VG} and n are
11used and each curve is associated with one of the DB classes. For the hydraulic conductivity
12curves, the Brooks and Corey model (Eq. (4)) was applied for water content lower than the
13value at $h=-20\text{ mm}$. Between this value and saturation a linear relationship between the
14natural logarithm of conductivity versus water content was assumed, as previously done to
15take into account the effect of macropores (Olioso *et al.*, 2002). A more comprehensive
16model, as the one proposed by Jarvis (2009) could be also be used to represent the sharp
17increase in hydraulic conductivity when moving from near-saturation to saturation.
18Then one curve should be drawn for the various possible combinations of DB and KS classes.
19Below -20 mm for h , and the corresponding value for θ , the curves $K(\theta)$ differ only due to
20differences in saturated water contents – the same value is used for the parameter η and there
21are only small differences between $K(-20\text{ mm})$ for a given DB class -. Therefore, only three
22curves can be distinguished, that correspond mainly to the DB classes, Between -20 mm of
23pressure and the saturation, the $K(\theta)$ curves differ also because of differences in the saturated

1

1hydraulic conductivity values K_s . Briefly, the water retention curve are only DB classes
2dependent and the hydraulic conductivity $K(\theta)$ are both DB and KS classes dependent.

3The differences in saturated hydraulic conductivities identified amongst land use are only
4influential on a small part of the curves, i.e very close to saturation. The accurate
5determination of saturated water content (and therefore of dry bulk density) is shown to be the
6most important point to get accurate description of soil hydraulic properties over the whole
7range of water content. As we have shown that dry bulk density is highly related to organic
8matter content, these differences can be assessed quite easily in the field.

9

10*Mapping of topsoil hydraulic properties*

11From the results presented previously, a preliminary mapping of topsoil hydraulic properties
12over the Mercier catchment can be proposed.

13In our case study, we have shown that the soil texture is quite homogeneous and that the
14variability of the shape parameters of the retention and hydraulic conductivity curves, n and
15 η , is low. As a first approximation, these parameters are assumed constant over the whole
16catchment. A more refined map could be obtained by mapping first the clay, sand, and silt
17contents, using for instance the kriging technique. The shape parameters n and η could then
18be derived from the soil texture, as done in this paper (see also Lassabatère *et al.*, 2006).

19The major outcome of our study is to show that soil porosity, saturated water content and
20saturated hydraulic conductivity, are mostly determined by land use. A land use map can
21therefore be used for the mapping of those parameters. In our study catchment, the land use
22field survey has shown that the accuracy of the Corine land cover map was too low to
23properly distinguish between the relevant land uses, especially crops. A more detailed land
24use map is therefore required. It can be derived from high resolution aerial photographs or
25satellite imagery. Such mapping is in progress on the Yzeron catchment (Béal *et al.*, 2009) but

1

1 was not available at the time of the field survey. For the Mercier catchment, a detailed map
2 was digitalized from aerial photographs (IGN BD ORTHO 2003, updated using the IGN BD
3 ORTHO 2008) and corrected using the cadastre for urbanised areas. This map was
4 reclassified for the representation of topsoil hydraulic properties. This classification combines
5 the DB classes of Table IV and the KS classes of Table VI. The correspondence between the
6 original land use map and the reclassified one is given in Table VII. The resulting map is
7 shown in Figure 9 where non sampled areas appear in white colour. For each DB-KS class,
8 one value of porosity, saturated water content and hydraulic conductivity can be affected
9 using for instance the average of the DB classes and the media of the KS classes (Table VII).

10

11 DISCUSSION

12

13 *Sampling strategy*

14 The sampling strategy is very important for an efficient mapping of the hydraulic parameters.
15 It has been pointed out as a key question by Park and van de Giesen (2004). The question of
16 sampling is especially relevant when dealing with a large catchment such as the Mercier
17 catchment (7 km²) (published studies are often related to catchments of less than 1 km²). In
18 previous works performed using the *Beerkan* method, on much larger catchments, a regular
19 grid sampling was used. Such a strategy was used during the EFEDA project on a 10x10 km²
20 area in Central Spain (Braud *et al.*, 2003). A regular grid (3.5 km resolution) complemented
21 by a transect with a 20 m spacing, was also used during a field campaign conducted in the
22 Donga catchment (580 km²) in Benin (Varado *et al.*, 2006). Analysis of the Benin data
23 showed a spatial correlation of about 50 to 100 m for the saturated hydraulic conductivity and
24 no correlation on the 3.5 km grid. On the other hand, it was shown that average values were
25 significantly different when the data were classified according to pedological units. A regular

1grid sampling does not allow the valorization of existing information such as pedology and
2land use. The sampling strategy adopted in this study was focused on the future hydrological
3modeling, where the hydrological units, coined as hydro-landscapes by Dehotin and Braud
4(2008), are chosen to be as homogeneous as possible with respect to soil, land use and other
5factors such as slope or the Beven topographic index. The pre-selection of sites based on the
6combination of pedology and land use information, as well as accessibility, was found
7efficient in terms of duration of the field campaign and use of human resources. It allowed the
8sampling of pedology/land use combinations representing a significant fraction of the
9catchment area. As shown in Figure 9, the characterization of artificialized areas is missing,
10but lots of practical problems (mainly difficult access to private properties) prevent an
11efficient sampling of these areas. As much as possible, the literature should be used instead.

12*Results of the infiltration tests*

13In this study two types of infiltration test were used to assess the hydraulic properties of the
14Mercier catchment topsoil A horizon. For a given location, the results of the three SR
15infiltration tests replications were in general very consistent whereas the variability was larger
16for the MDI infiltration tests. The difference in sampling surface between both devices may
17be the explanation. Indeed, the large cylinder diameter of the SR tests averaged most of the
18soil heterogeneity and removed much of the spatial variability due to inadequate sampling of
19macropore effect. The large diameter of the cylinder also filtered out the effects of terrain
20slope and vegetation. It reduces the effect of the heterogeneity of soil structure and texture
21and the parameters estimated from the infiltration tests are associated with this weighing of
22surface heterogeneities. The obtained values can therefore be considered representative of the
23field. On the other hand, the sampling surface of the MDI infiltrometer was very small and
24therefore these were much more sensitive to soil variability and heterogeneity of the topsoil A
25horizon. However, given the slope and the surface heterogeneity, it would have been difficult

1to use a large diameter for the mini-disk: this apparatus requires a flat surface to ensure
2stability and a good contact with the membrane. This would have required digging through
3the slope, that would have disturbed the soil surface and would not have been representative
4of the topsoil anymore. Finally, the two types of infiltration tests were complementary and
5well adapted to the field conditions on this highly structured soil.

6In addition, the positive head infiltration test allowed a characterization of saturated
7conditions, whereas the tension-disk data provided information on near-saturated hydraulic
8conductivity (-20 mm of water pressure), and illustrated the sharp increase in conductivity
9when moving from near-saturated to saturated conditions. This difference can be explained by
10the activation, at saturation, of a macropore network related to the high organic content, and a
11higher root system density and soil fauna activity in natural vegetations (broad leaved forest,
12permanent pasture). A review of the effect of macropores on water flow has been proposed by
13Beven and Germann (1982). They reports an increase of the infiltration capacity of soils with
14macropores. In the paper by Zhou *et al.* (2008, Table 5, Fig. 1), a ratio of about 10 between
15hydraulic conductivity at -30 mm of pressure and saturation is reported for woodland,
16cropland, pasture and urban land uses. In the paper by Schwartz *et al.* (2003, Fig. 3) the ratio
17between hydraulic conductivity at -20 mm of pressure and saturation is of about 2. In these
18two papers saturated hydraulic conductivity was obtained using tension-disk infiltrometers
19with a pressure of 0 m, which are shown by Reynolds *et al.* (2000) to provide lower estimates
20of saturated hydraulic conductivity than pressure infiltrometers Our values are therefore
21consistent with the literature, although the values of the ratio is around 50 in our study.

22

23The BEST method used in data interpretation was found robust and allowed us to obtain
24results even in adverse conditions (gentle slope, very rapid infiltration, and dense vegetation
25detritus cover in some cases). The strength of the method is its ability to exploit both the short

land long term ranges of the infiltration tests in order to describe at best the data. It also
provided physical results when traditional methods, based only on the short time infiltration
regime, failed. The method is applicable for both positive head and tension-disk infiltration
data, provided the contact layer has no significant influence on the early stages of infiltration.
When positive head is applied, the method provides an estimate of the normalization
parameter for the pressure and thus a complete description of both the retention and hydraulic
conductivity curves, which is not the case of traditional analysis methods. However, several
limitations of the methods have been identified. Xu et al. (2009) underline that the BEST
method is not effective when the initial water content is not sufficiently different from the
final water content. However, this restriction apply to all the methods of analysis because the
difference in water content appears in the denominator of Eq. (6). Another limitation is related
to the use of two different equations during the analysis which requires the determination of
the number of points where the small time infiltration equation is valid, through a specific
BEST routine (Eq. (7)). This choice influences the final sorptivity value and is therefore
important. The approximation provided by Eq.(6) was shown to be adequate for modeling
Beerkan infiltration experiments, provided its use is restricted to valid intervals (Lassabatere
et al., 2009). Improvement of the BEST method were recently proposed for specific soils
(Yilmaz et al., 2010) but were not used here. Based on the validation of the full integration
equation (Lassabatere et al., 2009), work is in progress in order to directly solve the full
infiltration equation proposed by Haverkamp et al. (1994). The results presented in the paper
were partly verified using this new solution, which strengthens the confidence in the
conclusions. More theoretical and numerical studies should be conducted to better assess the
impact of slope on the final results.

1Impact of land use on topsoil hydraulic properties

2Our study also highlighted the impact of land use on soil structural parameters, whereas the
3impact of pedology was not found so significant in our case study. Three land use classes
4were identified, leading to significant differences in dry bulk density and porosity. These
5classes were highly related to the organic matter content and therefore to the land use insofar
6as organic matter content is lower in cultivated lands than in natural areas (forests, permanent
7pastures). Lal (1996) reported an increase in dry bulk density when forest was replaced by
8cultivated lands, which is consistent with our findings.

9In our study, three further land use classes were identified with significant differences in
10saturated hydraulic conductivity and sorptivity. However, these classes were not significantly
11different in terms of near-saturated hydraulic conductivity, showing that the classes were
12probably related to macropores. Once again, the appearance of a dense macropore network is
13favoured by fauna activity and the dense root network in natural vegetations. Several authors
14have reported results showing the impact of land use on soil hydraulic properties. For
15instance, Marshall *et al.* (2009) report higher saturated hydraulic conductivity of soil beneath
16tree hedges than in agricultural fields, with a ratio of the both of about 3. Reynolds *et al.*
17(2000, Table 4) report values of saturated hydraulic conductivity measured using pressure
18infiltrimeters. The geometric mean values on natural woodlot are 2 to 10 times larger than
19those under conventional and no-tillage practices. More stable soil structure and increased
20biological activity might explain the larger hydraulic conductivity in forest, permanent pasture
21or minimum tillage systems (Bodhinayake and Si, 2004). Stolte *et al.* (2003) report that the
22permanent land use (forest, orchard, wasteland, shrub) showed a greater heterogeneity of
23saturated hydraulic conductivity than the arable areas and the values were significantly higher
24in permanent land use than in cultivated areas, as in our study. This was probably due to more
25macropores, associated with the activity of fauna and roots in the permanent system than in

1

1arable land. Such changes in topsoil hydraulic properties are very important for hydrological
2processes such as surface runoff but also groundwater, and water quality. They modify the
3hydrological response in terms of water balance components and their annual temporal
4variability (e.g., Fohrer *et al.*, 2005; Bormann *et al.*, 2007). Hibbert (1967) and Bosch and
5Hewlett (1982) concluded that a reduction of the forest cover increases water runoff.

6Our data were collected in autumn, but especially for agricultural fields, our results should be
7complemented by a monitoring of the time evolution of soil hydraulic properties, as suggested
8by several studies. This fact is especially relevant for agricultural fields where soil properties
9are modified regularly by agricultural practices such as ploughing, sowing, etc...(Zhou *et al.*,
102008; Bormann and Klassen, 2008; Le Bissonais *et al.*, 2005; Schwarts *et al.*, 2003; Mubarak
11*et al.*, 2009).

12

13CONCLUSIONS

14The results presented in this paper show that using an adequate spatial sampling taking into
15account pedology, and especially land use, it was possible to document the spatial variability
16of soil hydraulic properties of a small catchment of 7 km². The use of two types of infiltration
17tests, namely positive head and tension disk infiltration tests, combined with particle size data
18analysis and porosity measurements, allowed the derivation of estimates of the retention and
19hydraulic conductivity curves. Positive head and tension-disk data provided complementary
20information about saturated and near-saturated hydraulic conductivity of the topsoil A
21horizon. They highlighted a sharp increase of hydraulic conductivity when moving from
22near-saturated (-20 mm of water pressure) to saturated conditions. This fact could be related
23to the existence of macroporosity, mainly related to land use management. Therefore, the
24monitoring of both saturated and near-saturated hydraulic conductivity can provide
25information on the long term impact of land use on soil hydraulic properties.

1

In addition, the study revealed a significant impact of land use on dry bulk density and porosity, as well as on saturated hydraulic conductivity. This result opens perspectives for the spatialization of soil hydraulic conductivity. Traditionally, in distributed hydrological models, soil hydraulic properties are specified using pedo-transfer functions that rely mainly on soil texture and sometimes on porosity (or dry bulk density). These functions are generally fitted on a limited data set, often obtained in the laboratory, and might not be adapted to *in situ* soil conditions. Our study highlights the impact of land use on soil hydraulic properties and confirms the results of other authors such as those mentioned in the *Discussion* section. This should also be taken into account in the mapping of soil hydraulic properties for hydrological modelling. We have shown that a high resolution land use map is very valuable and can be used for this purpose.

12

13ACKNOWLEDGEMENTS

The soil data base was provided by SOL INFO RHONE-ALPES, sira@rhone-alpes.chambagri.fr, <http://www.rhone-alpes.chambagri.fr/sira/>. The study was funded by the French Agence Nationale de la Recherche (ANR) under contract n° ANR-07-VULN-1701. The stay of the first author at Cemagref was funded by Queretaro University, Mexico and Cemagref. Jean-Pierre Vandervaere provided useful comments on the interpretation of tension disk infiltration tests. We also thank two anonymous reviewers for their suggestions which help improve the quality of the paper.

21

22REFERENCES

Béal D, Gagnage M, Jacqueminet C, Kermadi S, Michel C, Jankowsky S, Branger F, Braud I. 2009. Cartographie de l'occupation du sol pour la modélisation hydrologique spatialisée du

1cycle de l'eau en zone péri-urbaine, Proceedings 2^{ème} atelier SIDE2009 Systèmes
2d'Informations et de Décision pour l'Environnement, Biramonte S, Miralles A, Pinet F (eds),
3Toulouse, France, May 26 2009, 10 pp. Available at [http://eric.univ-](http://eric.univ-lyon2.fr/~sbimonte/side2009.html)
4[lyon2.fr/~sbimonte/side2009.html](http://eric.univ-lyon2.fr/~sbimonte/side2009.html), consulted on 2010/01/15.

5Beven K, Germann P. 1982. Macropores and water flow in soils. *Water Resources Research*,
6**18(5)**: 1311-1325.

7Bodhinayake W, Si BC. 2004. Near-Saturated surface soil hydraulic properties under different
8land use in the St Denis National Wildlife Area, Saskathchewan, Canada. *Hydrological*
9*Processes* **18**: 2835-2850.

10Booth DB, Hartley D, Jackson R. 2002. Forest cover, impervious-surface area, and the
11mitigation of stormwater impacts. *Journal of the American Water Resources Association*,
12**38(3)**: 8356-845.

13Bormann H, Breuer L, Gräff T, Huisman JA. 2007. Analysing the effects of soil properties
14changes associated with land use changes on the simulated water balance: A comparison of
15three hydrological catchment models for scenario analysis. *Ecological Modelling*, **209(1)**: 29-
1640.

17Bormann H, Klassen K. 2008. Seasonal and land use dependent variability of soil hydraulic
18and soil hydrological properties of two Northern German soils. *Geoderma* **145**: 295-302.

19Bosch JM, Hewlett PM. 1982. A review of catchment experiments to determine the effect of
20vegetation changes on water yield and evapotranspiration. *Journal of Hydrology* **55**:3-23.

21Boulet G, Kalma JD, Braud I, Vauclin M. 1999. An assessment of effective parameterization
22of soil physical and land surface properties in regional-scale water balance studies. *Journal of*
23*Hydrology* **217**: 225-238.

24Bras RL, Perkins FE. 1975. Effects of urbanization on catchment response. *J. of Hydraulics*
25*Division* **101** HY3: 451-466.

- 1Braud I. 1998. Spatial variability of surface properties and estimation of surface fluxes of a
2savannah. *Agricultural and Forest Meteorology* **89(1)**: 15-44.
- 3Braud I, de Condappa D, Soria J, Haverkamp R, Angulo-Jaramillo R, Galle S, Vauclin M.
42005. Use of scaled forms of the infiltration equation for the estimation of unsaturated soil
5hydraulic properties (Beerkan method). *European Journal of Soil Science* **56**: 361-374. DOI:
610.1111/j.1365_2389.2004.00660.x.
- 7Braud I, Haverkamp R, Arrué JL, Lopez MV. 2003. Spatial variability of soil surface
8properties and consequences on the annual and monthly water balance of a semi-arid
9environment (EFEDA experiment). *Journal of Hydrometeorology* **4(1)**: 121-137.
- 10Brooks RH, Corey CT. 1964. Hydraulic properties of porous media. *Hydrological Paper* **3**.
11Colorado State University, Fort Collins, CO.
- 12Burdine NT. 1953. Relative permeability calculations from pore size distribution data.
13*Transactions of the American Institute of Mining, Metallurgical, and Petroleum Engineers*
14**198**: 71-77.
- 15Chen L, Young MH. 2006. Green-Ampt infiltration model for sloping surfaces. *Water*
16*Resources Research* **42**: W07420, doi:10.1029/2005WR004468
- 17Childs EC, Collis-George C. 1950. The permeability of porous media. *Proceedings of the*
18*Royal Society London Series A* **201**: 393-405.
- 19Chocat B, Krebs P, Marsalek J, Rauch W, Schilling W. 2001. Urban drainage redefined: from
20stormwater removal to integrated management. *Water and Science Technology* **43**:61-68.
- 21Clapp RB, Hornberger GM. 1978. Empirical equations for some soil hydraulic properties.
22*Water Resources Research* **14(4)**: 601-604.
- 23Cosby BJ, Hornberger, GM, Clapp RB, Ginn TR. 1984. A statistical exploration of the
24relationships of soil moisture characteristics to the physical properties of soils. *Water*
25*Resources Research* **20(6)**: 682-690.

1de Condappa D. 2005. Etude de l'écoulement d'eau à travers la zone non-saturée des aquifères
2de socle à l'échelle spatiale du bassin versant. Application à l'évaluation de la recharge au sein
3du bassin versant de Maheshwaram, Andhra Pradesh, Inde, Université Joseph Fourier,
4Grenoble, France, 22 Avril 2005, 355 pp.

5de Souza ES, Antonino ACD, Angulo-Jaramillo RA, Netto AM, Montenegro SMGL, da Silva
6EB. 2008. Spatial variability of hydrodynamic parameters in two agricultural plots in Paraíba
7state – Brazil, *Reivista, Brasileira de ciencia do solo* **32(5)**: 1795-1804.

8Dehotin J, Braud I. 2008. Which spatial discretization for distributed hydrological models?
9Proposition of a methodology and illustration for medium to large scale catchments.
10*Hydrology and Earth System Sciences* **12**: 769-796.

11Desbordes M. 1989. Principales causes d'aggravation des dommages dus aux inondation par
12ruissellement superficiel en milieu urbanisé. *Bulletin hydrologie urbaine*- SHF, Paris, **4** : 2-
1310.

14Fohrer N, Haverkhamp S, Frede H. 2005. Assessment of the effects of land use patterns on
15hydrological landscape functions: development of sustainable land use for low mountain
16range areas. *Hydrological Processes* **19** : 659-672.

17Gnouma R. 2006. Aide à la calibration d'une modèle hydrologique distribué au moyene d'une
18analyse des processus hydrologiques: application au bassin versant de l'Yzeron. Thèse
19Doctoral. Institut National des Sciences Appliquées de Lyon. France, 412 pp.

20Gutmann ED, Small EE. 2005. The effect of soil hydraulic properties versus soil texture in land
21surface models. *Geophysical Research Letters* **32**: L02402, doi: 10.1029/2004GL021843.

22Haverkamp R, Bouraoui F, Angulo-Jaramillo R, Zammit C, Delleur JW. 1998. Soil properties
23and moisture movement in the unsaturated zone. In: *CRC Groundwater Engineering*
24*Handbook*, Delleur JW (ed), CRC Press, Boca Raton, Florida: 5.1-5.50,.

- 1Haverkamp R, Leij FJ, Fuentes C, Sciortino A, Ross PJ. 2005. Soil water retention: I.
- 2Introduction of a shape index. *Soil Science Society of America Journal* **69**: 1881-1890, doi:
- 310.2136/sssaj2004.0225.
- 4Haverkamp R, Ross PJ, Smettem KRJ, Parlange JY. 1994. Three-dimensional analysis of
- 5infiltration from the disk infiltrometer 2. Physically based infiltration equation. *Water*
- 6*Resources Research* **30(11)**: 2931-2935.
- 7Herman S, Mertens J, Timmerman A, Feyen J. 2003. Comparison of tension infiltrometer,
- 8single-ring pressure infiltrometer and soil core Ksat estimates on a sandy loam hillslope. EGS
- 9- AGU - EUG Joint Assembly, Abstracts from the meeting held in Nice, France, 6 - 11 April
- 10Hibbert AR. 1967. Forest treatment effects on water yield. In the International Symposium
- 11on Forest Hydrology, Pennsylvania , September 1965, Sopper WE, Lull HW (eds.) Pergamon;
- 12Oxford.
- 13Islam N, Wallender WW, Mitchell JP, Wicks S, Howitt RE. 2006. Performance evaluation of
- 14methods for the estimation of soil hydraulic parameters and their suitability in a hydrologic
- 15model. *Geoderma* **134(1-2)**: 135-151.
- 16Jarvis N. 2009. Near-saturated hydraulic properties of macroporous soils. *Vadose Zone*
- 17*Journal* **7**: 1302-1310.
- 18Lafont M, Vivier A, Nogueira S, Namour P, Breil P. 2006. Surface and hyporheic oligochaete
- 19assemblages in a French suburban stream. *Hydrobiologia* **564(1)**: 183-193.
- 20Lal R. 1996. Deforestation and land-use effects on soil degradation and rehabilitation in
- 21western Nigeria. I. Soil physical and hydrological properties. *Land degradation and*
- 22*development* **7**: 19-45.
- 23Lassabatère L, Angulo-Jaramillo R, Soria Ugalde JM, Cuenca R, Braud I, Haverkamp R.
242006. Beerkan estimation of soil transfer parameters through infiltration experiments. *Soil*
- 25*Science Society of America Journal* **70**: 521-532.

- 1Lassabatère L, Angulo-Jaramillo R, Soria Ugalde JM, Simunek J, Haverkamp R. 2009.
- 2Analytical and numerical modeling of water infiltration experiments. *Water Resources*
- 3*Research* **45**: W12415.
- 4Le Bissonnais Y, Cerdan O, Lecomte V, Benkhadra H, Souchere V, Martin P. 2005.
- 5Variability of soil surface characteristics influencing runoff and interrill erosion. *Catena* **62**:
- 6111-124.
- 7Marsalek J, Jiménez-Cisneros BE, Karamouz M, Malmquist PA, Gldenfum J, Chocat B.
82007. Urban water processes and interactions. UNESCO IHP-VI program, UNESCO, Paris,
- 9239 pp.
- 10Marshall MR, Francis OJ, Frobrook ZL, Jackson BM, McIntyre N, Reynolds B, Solloway I,
- 11Weather HS, Chell J. 2009. The impact of upland land management on flooding: results from
- 12an improved pasture hillslope. *Hydrological Processes* **23**: 464-474.
- 13Matteo M, Randhir T, Bloniarz D. 2006. Watershed-scale impacts of forest buffers on water
- 14quality and runoff in urbanizing environment. *Journal of the American Water Resources*
- 15*Association* **132**:144-152.
- 16Mualem Y. 1976. A new model for predicting the hydraulic conductivity of unsaturated
- 17porous media. *Water Resources Research* **12**, 513-522.
- 18Mubarak I, Mailhol JC, Angulo-Jaramillo R, Ruelle P, Khaledian M. 2009. Temporal
- 19variability in soil hydraulic properties under drip irrigation. *Geoderma* **150(1-2)**: 158-165
- 20doi:10.1016/j.geoderma.2009.01.022.
- 21Oliosio A, Braud I, Chanzy A, Courault D, Demarty J, Kergoat L, Lewan E, Ottlé C, Prévot L,
- 22Zhao W, Calvet JC, Cayrol P, Jongschaap R, Moulin S, Noilhan J, Wigneron JP. 2002. SVAT
- 23modelling over the Alpilles-ReseDA experiment: comparing SVAT models over wheat fields.
- 24*Agronomie* **22**: 651-668.
- 25OTHU, 2010. <http://www.graie.org/othu/>. Consulted on 2010/01/06.

- 1Park SJ, van de Giesen N. 2004. Soil-landscape delineation to define spatial sampling
2domains for hillslope hydrology. *Journal of Hydrology* **295**(1-4): 28-46.
- 3Philip JR. 1969. Theory of infiltration. *Advances in Hydrosience* **5**: 215-296.
- 4R Development Core Team, 2004.R: a language and environment for statistical computing. R
5foundation for statistical computing. Vienna, Austria. <http://www.r-project.org/>. Consulted on
62010/01/06.
- 7Radojevic B. 2002. Méthode d'évaluation de l'influence urbaine sur le régime des crues d'un
8bassin versant de 130 km². Institut National des Sciences Appliquées de Lyon, Lyon.
- 9Randhir T. 2003. Watershed-scale effects of urbanization on sediment export: assesement
10and policy, *Water Resources Research* **39**(6), 1-13.
- 11Rawls WJ, Brakensiek DL. 1985. Prediction of soil water properties for hydrologic
12modelling. In: *E.B.a.W.* Jones TJ (eds), *Watershed Management in the eighties*. ASCE,
13Denver, April 30-May 1: 293-299.
- 14Reynolds WD, Bowman BT, Brunke RR, Drury CF, Tan CS. 2000. Comparison of tension
15infiltrometer, and soil core estimates of saturated hydraulic conductivity. *Soil Science Society*
16*of America Journal* **64**:478-484.
- 17Rogowski AS. 1971. Watershed physics: model of soil moisture characteristic, *Water*
18*Resources Research* **12**: 513-522.
- 19Scalenghe R, Ferraris S. 2009. The First Forty Years of a Technosol. *Pedosphere* **19**(1): 40-
2052.
- 21Schmitt L, Grosprêtre L, Breil P, Lafont M, Vivier A, Perrin JF, Namour P, Jezequel C,
22Valette L, Valin K, Cordier R, Cottet M. 2008. Préconisations de gestion physique de petits
23hydro systèmes périurbains : l'exemple du bassin de l'Yzeron (France). In. Actes du Colloque
24« La gestion physique des cours d'eau : bilan d'une décennie d'ingénierie écologique »,

1 Verniers G, Petit F (eds), Namur, 10-12 oct. 2007, Groupe Interuniversitaire de Recherches en
2 Ecologie Appliquée, Laboratoire d'Hydrographie et de Géomorphologie Fluviale, Direction
3 des Cours d'Eau Non Navigables, Direction Générale des Ressources Naturelles et de
4 l'Environnement - Ministère de Région wallonne : 177-186.

5 Schwarts R, Evett SR, Paul UW. 2003. Soil hydraulic properties of cropland compared with
6 reestablished and native grassland. *Geoderma* **116**: 47-60.

7 SIRA, 2010. Sol Info Rhône-Alpes, sira@rhone-alpes.chambagri.fr - [http://www.rhone-](http://www.rhone-alpes.chambagri.fr/sira/)
8 [alpes.chambagri.fr/sira/](http://www.rhone-alpes.chambagri.fr/sira/). Consulted on 2010/01/06.

9 Smettem KRJ, Parlange JY, Ross PJ, Haverkamp R. 1994. Three-dimensional analysis of
10 infiltration from the disk infiltrometer. 1. A capillary-base theory, *Water Resources Research*
11 **30**, 2925-2929.

12 Smiles DE, Knight JH. 1976. A note on the use of the Philip infiltration equation, *Australian*
13 *Journal of Soil Science* **10**: 143-150.

14 Sobieraj JA, Elsenbeer H, Vertessy RA. 2001. Pedotransfer functions for estimating saturated
15 hydraulic conductivity: implications for modelling storm flow generation. *Journal of*
16 *Hydrology* **251**: 202-220.

17 SOeS, 2010. Service de l'Observation et des Statistiques, Occupation des Sols, Corine Land
18 Cover, [http://www.ifen.fr/bases-de-donnees/occupation-des-sols-corine-land-cover.html?](http://www.ifen.fr/bases-de-donnees/occupation-des-sols-corine-land-cover.html?taille=)
19 [taille=](http://www.ifen.fr/bases-de-donnees/occupation-des-sols-corine-land-cover.html?taille=). Consulted on 2010/01/06.

20 Stolte J, van Venrooij B, Zhang G, Trouwborst KO, Liu G, Ritsema CJ, Hessel R. 2003.
21 Land-use induced spatial heterogeneity of soil hydraulic properties on the Loess Plateau in
22 China. *Catena* **54**: 59-75.

23 van der Keur P, Iversen BV. 2006. Uncertainty in soil physical data at the basin scale - a
24 review. *Hydrology and Earth System Sciences* **18**: 889-902

- 1Ivan Genuchten MT. 1980. A closed-form equation for predicting the hydraulic conductivity
2of unsaturated soils. *Soil Science Society of America Journal* **44** : 892-898.
- 3Vandervaere JP, Vauclin M, Elrick DE. 2000a. Transient flow from tension infiltrometers: I.
4The two-parameter equation. *Soil Science Society of America Journal* **64**: 1263-1272.
- 5Vandervaere JP, Vauclin M, Elrick DE. 2000b. Transient flow from tension infiltrometers: II.
6Four methods to determine sorptivity and conductivity. *Soil Science Society of America*
7*Journal*, **64**: 1271-1284.
- 8Varado N, Braud I, Galle S, Le Lay M, Séguis L, Kamagate B, Depaetere C. 2006. Multi-
9criteria assessment of the Representative Elementary Watershed approach on the Donga
10catchment (Benin) using a downward approach of model complexity. *Hydrology and Earth*
11*System Sciences* **10**: 427-442.
- 12Verecken H, Maes J, Darius P, Feyen J. 1989. Estimating the soil moisture retention
13characteristics from texture, bulk density and carbon content. *Soil Science* **148**: 389-404.
- 14Wösten JHM. 1997. Pedotransfer functions to evaluate soil quality; In *Development in soils*
15*sciences*, Gregorich E, Carter MR (eds)., Elsevier: Amsterdam; 221-245.
- 16Wösten JHM, Lilly A, Nemes A, Le Bas C. 1999. Development and use of a database of
17hydraulic properties of European soils. *Geoderma* **90**: 169-185.
- 18Wösten JHM, Pachepsky YA, Rawls WJ. 2001. Pedotransfer functions: bridging the gap
19between available basic soil data and missing soil hydraulic characteristics. *Journal of*
20*Hydrology* **251**: 123-150.
- 21Xu X, Kiely G, Lewis C. 2009. Estimation and analysis of soil hydraulic properties through
22infiltration experiments: comparison of BEST and DL fitting methods. *Soil Use and*
23*Management* **25**: 354-361.
- 24Yilmaz D, Lassabatère L, Angulo Jaramillo R, Legret M. 2010. Hydrodynamic
25characterization of BOF slags through adapted BEST method. *Vadoze Zone Journal* **9**: 1-10.

1

1Zhou X, Lin HS, White HS. 2008. Surface soil hydraulic properties in four soil series un
2different land uses and their temporal changes. *Catena* **73**: 180-188.

1

1

List of Figures

2

3Figure 1: Location of the Yzeron catchment and of the two experimental sub-catchments
4(Mercier and Chaudanne). The grey scale shows the catchment slope with the highest values
5in dark and the lowest values in white. The symbols indicate the location of rainfall (points)
6and streamflow gauges (triangles).

7Figure 2: Pedology map of the Mercier catchment (from Sol Info Rhône Alpes, SIRA, 2010).
8The various colors correspond to the various Soil Cartographic Units defined in Table I. The
9symbols show the location of the infiltration test sites, with the various symbols
10corresponding to the various land use defined in Table I.

11Figure 3: (a) Box plot of the fine particle size fractions and organic matter content (b) Box
12plot of the dry bulk density and porosity of the topsoil. On the box plots, boundaries indicates
13median, 25th and 75th quantiles, the top and bottom whiskers indicate the 10th and 90th
14percentiles and the points the minimum and maximum values.

15Figure 4: Presentation of the sampled points in the USDA textural triangle. The various
16symbols correspond to the different soil pedological units as defined in Table I.

17Figure 5: (a) Comparison of dry bulk density as measured using a 0-2.5 cm and 0-5 cm height
18cylinder. (b) Relationship between dry bulk density and organic matter content.

19Figure 6. Observed (points) and fitted cumulative infiltration data for sites 41.1 (clearing) and
2031-3 (orchards). The full line is the fit of Eq. (6) for short time steps and the dashed line is the
21fit of Eq. (10) for large time steps. Eq. (6) was fitted to the points plotted with squares.

22Figure 7. Box plots of saturated hydraulic conductivity (single ring) and hydraulic
23conductivity at -20 mm (mini-disk) for all the samples and the three identified classes KS1,
24KS2 and KS3.

1

Figure 8. Estimated retention curves and hydraulic conductivity curves for the combination of
classes DB1, DB2, DB3. Between near-saturated and saturated hydraulic conductivity, a
linear relationship on the natural logarithm of hydraulic conductivity versus soil water content
was assumed. The symbols are the saturated hydraulic conductivities for the various
combinations of DB and KS classes: broad leaved forest (DB1-KS1); coniferous forest (DB1-
KS3); permanent pasture (DB2-KS3); clearing (DB2-KS2); small woods (DB2-KS1);
cultivated pasture (DB3-KS2); crops (DB3-KS3)..

Figure 9. Mapping of soil hydraulic properties. The classes numbering is provided in Table
VII. White surfaces correspond to the non sampled areas defined in Table VII.

10

11

12

13

14

1

1Table I. Number of sampled points for Single Ring (SR) and Mini-Disk (MDI) infiltration
2tests per Soil Cartographic Unit (SCU) and land use (figures in parentheses are the percentage
3of the total number of points). In the land use classes, we distinguish between “permanent
4pasture” (in place for more than 5 years) and “cultivated pasture” (in place for only one or a
5few years).

SCU number or land use	Number of SR tests	Number of MDI
102 Loamy sand and clayey sand from gneiss and micaschist	15 (26%)	10 (23%)
1031 Loamy sands from tuf within a forest dominated by coniferous	6 (10%)	7 (16%)
7021 Loamy sands and clayey sands from colluvionated gneiss	15 (26%)	11 (25%)
704 Colluvions loamy sand to clayey sand with slope	6 (10%)	4 (9%)
7041 Colluvions loamy sand to clayey sand within talwegs	9 (16%)	5 (12%)
7042 Alluvions clayey-sands to sandy clays within talwegs and narrow valleys	7 (12%)	6 (14%)
Total	58	43
1 Permanent pasture	21 (36%)	14 (32%)
2 Cultivated pasture	9 (15%)	7 (16%)
3 Crop (wheat stubble)	3 (5%)	2 (5%)
4 Crop (bare soil after ploughing)	4 (7%)	3 (7%)
5 Orchards (peach, apples)	3 (5%)	2 (5%)
6 Broad-leaved forest (oaks, chestnuts)	6 (10%)	6 (14%)
7 Clearing	4 (7%)	2 (5%)
8 Coniferous forest	4 (7%)	4 (9%)
9 Small wood sometimes with ivy	4 (7%)	3 (7%)
Total	58	43

6

1

1Table II. Statistics of particle size data analysis, organic matter and shape parameters of the
2retention and hydraulic conductivity curves, n and η . CV is the coefficient of variation. The
3sample size is 28. Std stands for standard deviation

	Clay content	Fine silt content	Coarse silt content	Fine sand content	Coarse sand content	Organic matter content	n	η
Unit	%	%	%	%	%	g kg ⁻¹	-	-
Average	12.9	11.7	8.2	17.9	49.6	56.5	2.17	15.2
Std	4.0	3.5	2.5	3.6	10.4	26.9	0.045	3.2
Minimum	5.6	4.8	3.7	10.6	30.2	18.2	2.10	10.7
Maximum	22.7	20.1	13.7	23.8	73.4	133.0	2.26	22.8
CV (%)	13.8	29.9	30.5	20.1	21.0	47.6	2.1	21.0

4

5

1

1Table III. Average and standard deviation (std in parentheses) organic matter content, dry bulk density, porosity, sorptivity and hydraulic
2conductivity derived from the single ring (SR) infiltration tests in terms of land use class.

Land use	Sample size OM	Organic matter content	Sample size dry bulk density and SR	Dry bulk density	Porosity	Sorptivity SR	Saturated hydraulic conductivity SR
Units	-	g kg ⁻¹	-	kg m ⁻³	-	mm s ^{-1/2}	mm s ⁻¹
Permanent pasture	11	61.3 (10.9)	21	969 (122)	0.63 (0.05)	3.15 (2.45)	0.51 (0.75)
Cultivated pasture	4	35.6 (12.9)	9	1269 (305)	0.52 (0.11)	1.64 (0.58)	0.11 (0.08)
Crops (wheat stubble)	1	19.5 (NA)	3	1411 (24)	0.47 (0.01)	2.8 (0.76)	0.28 (0.10)
Crops (bare soil after ploughing)	1	18.2 (NA)	4	1549 (265)	0.41 (0.10)	0.84 (0.83)	0.13 (0.21)
Orchards (peach, apple)	1	28.3 (NA)	3	1472 (225)	0.44 (0.08)	3.62 (2.10)	0.40 (0.27)
Broad-leaved forest	3	88.8 (54.1)	6	676 (146)	0.74 (0.05)	4.86 (1.45)	1.32 (0.57)
Clearing	3	51 (21.2)	4	1180 (283)	0.55 (0.11)	1.16 (0.40)	0.05 (0.02)
Coniferous forest	1	84.5 (NA)	4	725 (130)	0.73 (0.05)	1.50 (0.91)	0.23 (0.15)
Small wood sometimes with ivy	3	65 (19.3)	4	1058 (292)	0.60 (0.11)	5.77 (2.12)	1.50 (0.62)
All	28	56.5 (26.6)	58	1078 (318)	0.59 (0.12)	2.87 (2.18)	0.50 (0.67)

3

1

Table IV. Statistics of organic matter content, dry bulk density, porosity and ratio (final water content/porosity) for the three main land use classes where significant differences were identified: class DB1: broad leaved forest + coniferous forest, class DB2: permanent pasture + clearing + small woods, class DB3: cultivated pasture + crop (wheat stubble) + crop (bare soil after ploughing) + orchards. Std stands for standard deviation

	Units	Number of samples	Organic matter	Dry bulk density	Porosity	Ratio final water content / porosity
		(-)	(g kg ⁻¹)	(kg m ⁻³)	(-)	(-)
Class DB1	Average	10	103.0	695	0.74	0.66
	(Std)		(24.4)	(135)	(0.05)	(0.16)
	[Min-Max]	-	[62.6-133]	[472-817]	[0.69-0.82]	[0.32-0.81]
Class DB2	Average	29	60.5	1010	0.62	0.69
	(Std)		(13.6)	(185)	(0.07)	(0.17)
	[Min-Max]	-	[26.5-86.3]	[685-1424]	[0.46-0.74]	[0.30-1.0]
Class DB3	Average	19	30.7	1382	0.48	0.70
	(Std)		(12.3)	(270)	(0.10)	(0.18)
	[Min-Max]	-	[18.2-53.3]	[846-1852]	[0.30-0.68]	[0.35-1.0]

5

6

1

1Table V. Statistics of maximum infiltrated depth, I_{max} , maximum infiltration time, t_{max} , and
2their ratio, L , for the single ring infiltration tests

Variable	Average (-)	Standard deviation (-)	Minimum (-)	Maximum (-)	Median (-)	Coefficient of variation (-)	Sample size
I_{max} (mm)	86.6	18.1	11.5	114.4	90	0.21	58
t_{max} (min)	10.3	19.3	0.25	114.4	2.95	1.87	58
L (mm min ⁻¹)	55.9	79.6	0.36	340	26.7	1.42	58

1

1Table VI. Statistics of sorptivity S , S , saturated hydraulic conductivity, sorptivity MDI, hydraulic conductivity at -20mm for the three main land
2use classes where significant differences were identified: class KS1: broad leaved forest + small woods, class KS2: cultivated pasture + crop
3(bare soil after ploughing) + clearing, class KS3: permanent pasture + crop (wheat stubble) + coniferous forest + orchard. Std stands for standard
4deviation.

5

		Number of samples SR	S (mm s ^{-1/2})	K_s (mm s ⁻¹)	h_{VG} (mm)	Number of samples MDI	$S(h=-20\text{mm})$ (mm s ^{-1/2})	$K_s(h=-20\text{mm})$ (mm s ⁻¹)	$K_s/K_s(h=-20\text{mm})$ (-)
	Units	(-)				(-)			(-)
Class KS1	Average	10	5.22	1.39	-72.2	7	0.08	0.0031	448
	(Std)		(1.70)	(0.56)	(56.5)		(0.05)	(0.0027)	
	Median		4.64	1.20	-55.2		0.10	0.0021	571
	CV (%)		32.6	40.3	78.2		62.5	87.1	
Class KS2	Average	17	1.34	0.10	-74.0	12	0.11	0.0039	26
	(Std)		(0.67)	(0.11)	(60.3)		(0.05)	(0.0028)	
	Median		1.20	0.06	-65.5		0.10	0.0029	21
	CV (%)		50.0	110.0	81.5		45.4	71.8	
Class KS3	Average	30	2.95	0.44	-63.5	20	0.10	0.0075	59
	(Std)		(2.18)	(0.63)	(41.8)		(0.05)	(0.0067)	
	Median		2.47	0.24	-64.7		0.09	0.0049	49
	CV (%)		73.9	143.2	65.8		50.0	89.3	
All	Average	57	0.59	2.87	-68.1	37	0.10	0.0056	515
	(Std)		(0.12)	(2.18)	(49.8)		(0.052)	(0.0054)	
	Median		2.05	0.22	-64.8		0.10	0.0047	47
	CV (%)		20.3	76.0	73.1		52.0	96.7	

6

2

48

1

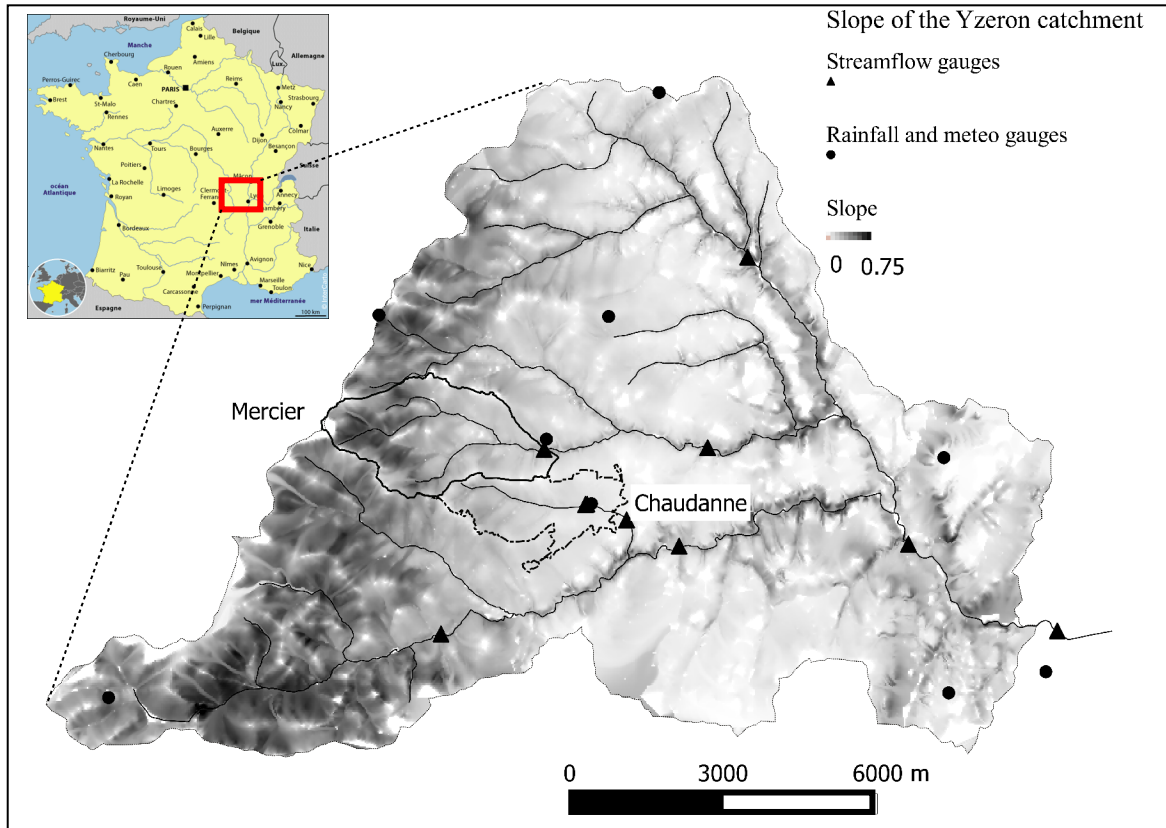
1Table VII. Correspondence between the original detailed land use map of the Mercier catchment and the reclassified map according to the dry
2bulk (DB) and saturated hydraulic conductivity (KS) classes for mapping of porosity, saturated water content and saturated hydraulic
3conductivity.

Reclassified land use class	Original classes of the Mercier land use map	Porosity (-)	Saturated water content ($\text{m}^3 \text{m}^{-3}$)	Near saturated hydraulic conductivity (-20 mm pressure) (mm s^{-1})	Saturated hydraulic conductivity (mm s^{-1})
DB1-KS1 (11)	Broad-leaved forest,	0.74	0.49	0.0031	1.39
DB1-KS3 (13)	Coniferous forest	0.74	0.49	0.0075	0.44
DB2-KS1 (21)	Scattered trees, hedges,	0.62	0.43	0.0031	1.39
DB2-KS2 (22)	Moors, heathland, fallow land,	0.62	0.43		
DB2-KS3 (23)	Pasture	0.62	0.43	0.0075	0.44
DB3-KS2 (32)	Ploughed fields, scattered grass,	0.48	0.34		
DB3-KS3 (33)	Orchards, berry plantation, wasteland, dump sites, spaces under construction, cemeteries	0.48	0.34	0.0075	0.44
Not sampled during the campaign	Impermeable surface (cement, asphalt), road networks, dirt roads, pervious artificial surfaces (gardens, trees)	Literature	Literature	Literature	Literature
Not relevant	Water bodies	NA	NA	NA	NA

4

1

1



2

Figure 1: Location of the Yzeron catchment and of the two experimental sub-catchments (Mercier and Chaudanne). The grey scale shows the catchment slope with the highest values in dark and the lowest values in white. The symbols indicate the location of rainfall (points) and streamflow gauges (triangles).

1

1

2

3

4

5

6

7

8

9

10

11

12

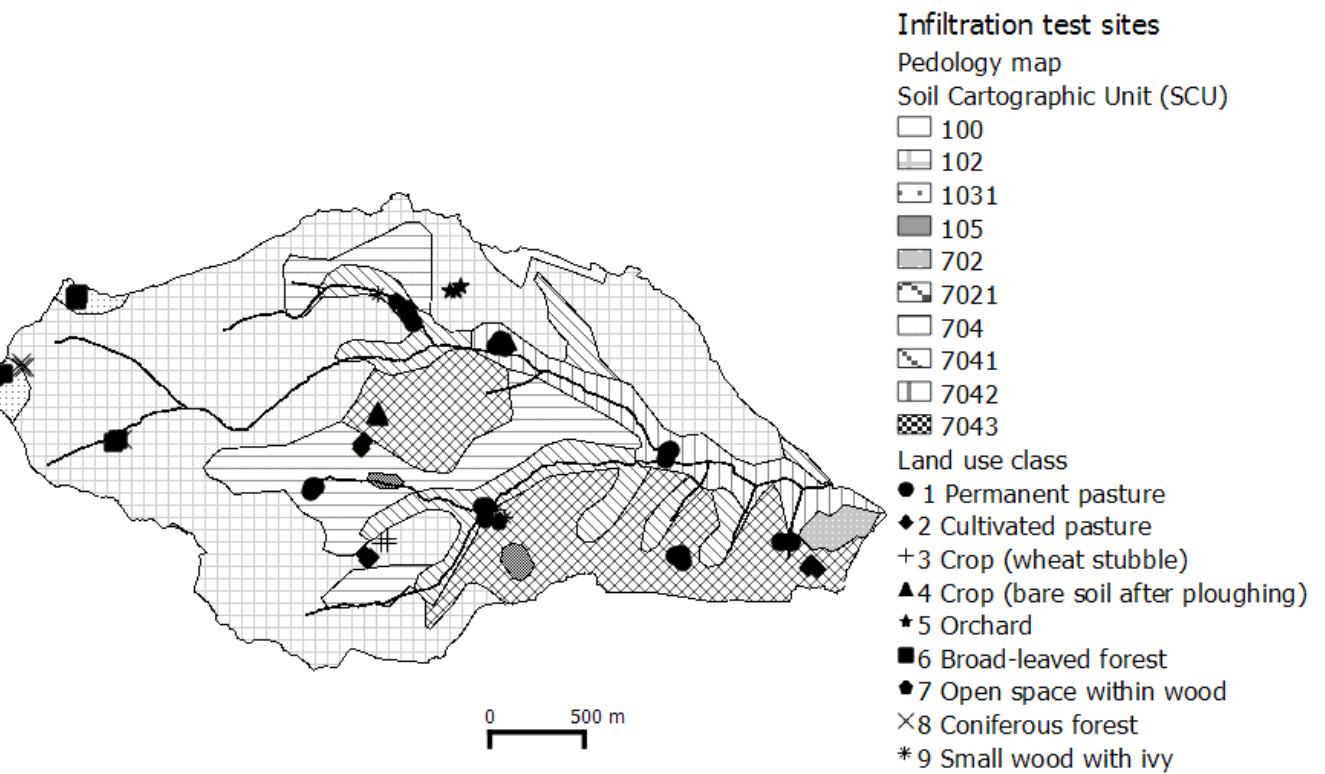
13

14

15

16

17



18Figure 2: Pedology map of the Mercier catchment (from Sol Info Rhône Alpes

19<http://www.rhone-alpes.chambagri.fr/sira/>). The various colors correspond to the various Soil

20Cartographic Units defined in Table I. The symbols show the location of the infiltration test

21sites, with the various symbols corresponding to the various land use defined in Table I

22

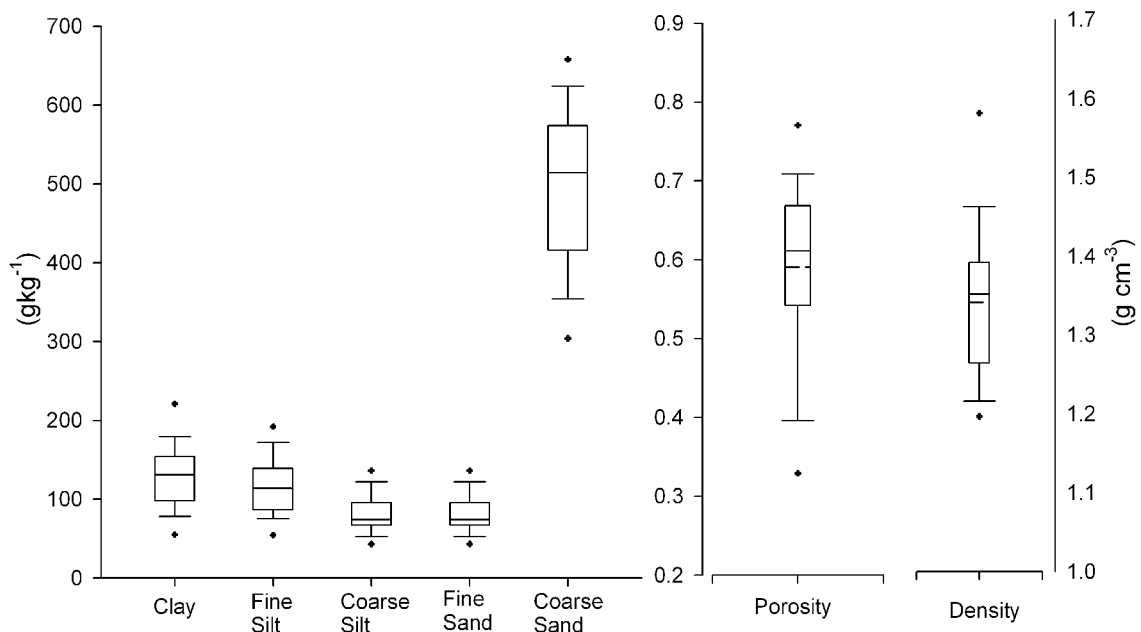
23

24

25

1

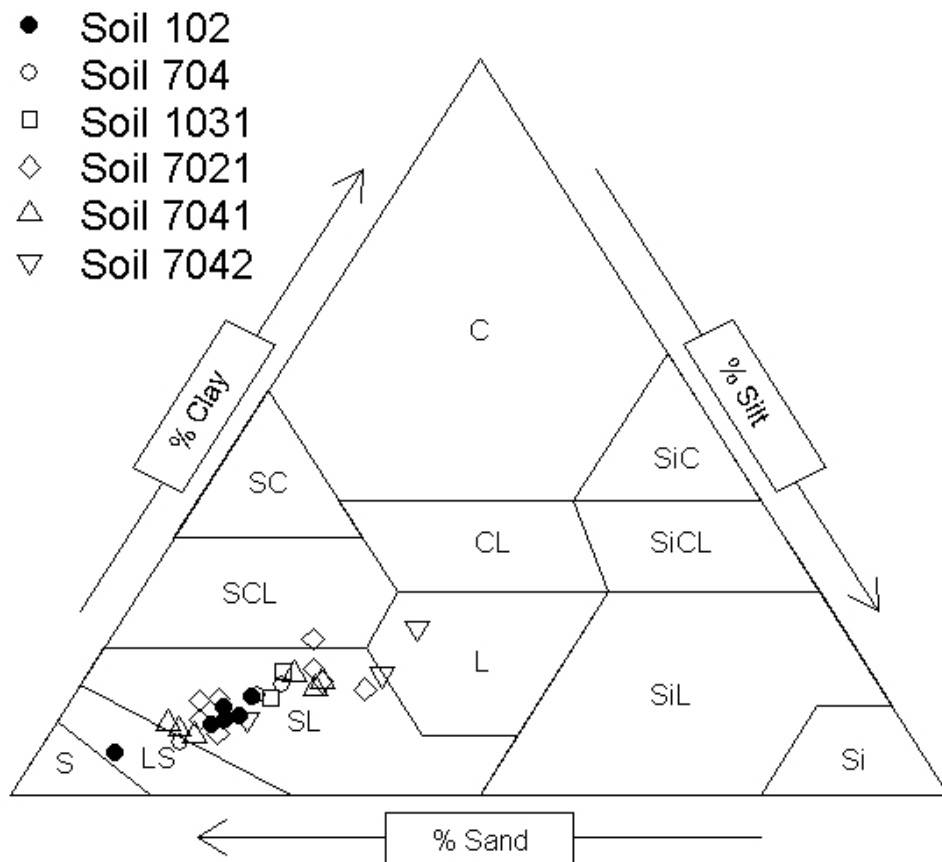
1



2

Figure 3: (a) Box plot of the fine particle size fractions and organic matter content (b) Box plot of the dry bulk density and porosity of the topsoil. On the box plots, boundaries indicates median, 25th and 75th quantiles, as vertical boxes error bars respectively: the top and bottom whiskers indicate the 10th and 90th percentiles and the points the minimum and maximum values.

1

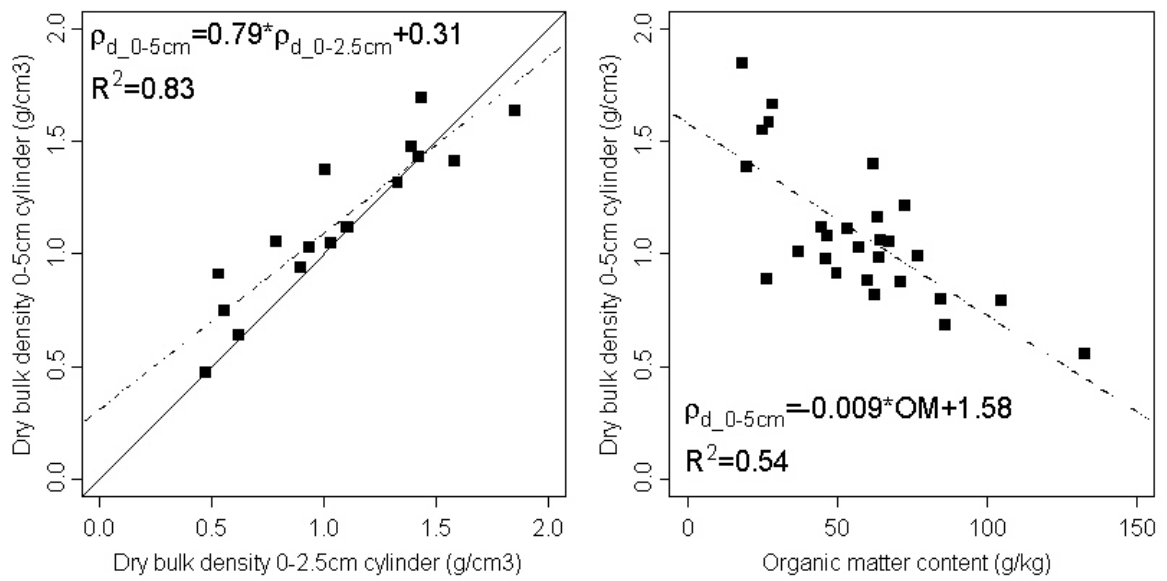


1

2

3 Figure 4: Presentation of the sampled points in the USDA textural triangle. The various
4 symbols correspond to the different soil pedological units as defined in Table I..

1



1

2Figure 5: (a) Comparison of dry bulk density as measured using a 0-2.5 cm and 0-5 cm height
3cylinder. (b) Relationship between dry bulk density and organic matter content.

1

1

2

3

4

5

6

7

8

9

10

11

12

13

14

15

16

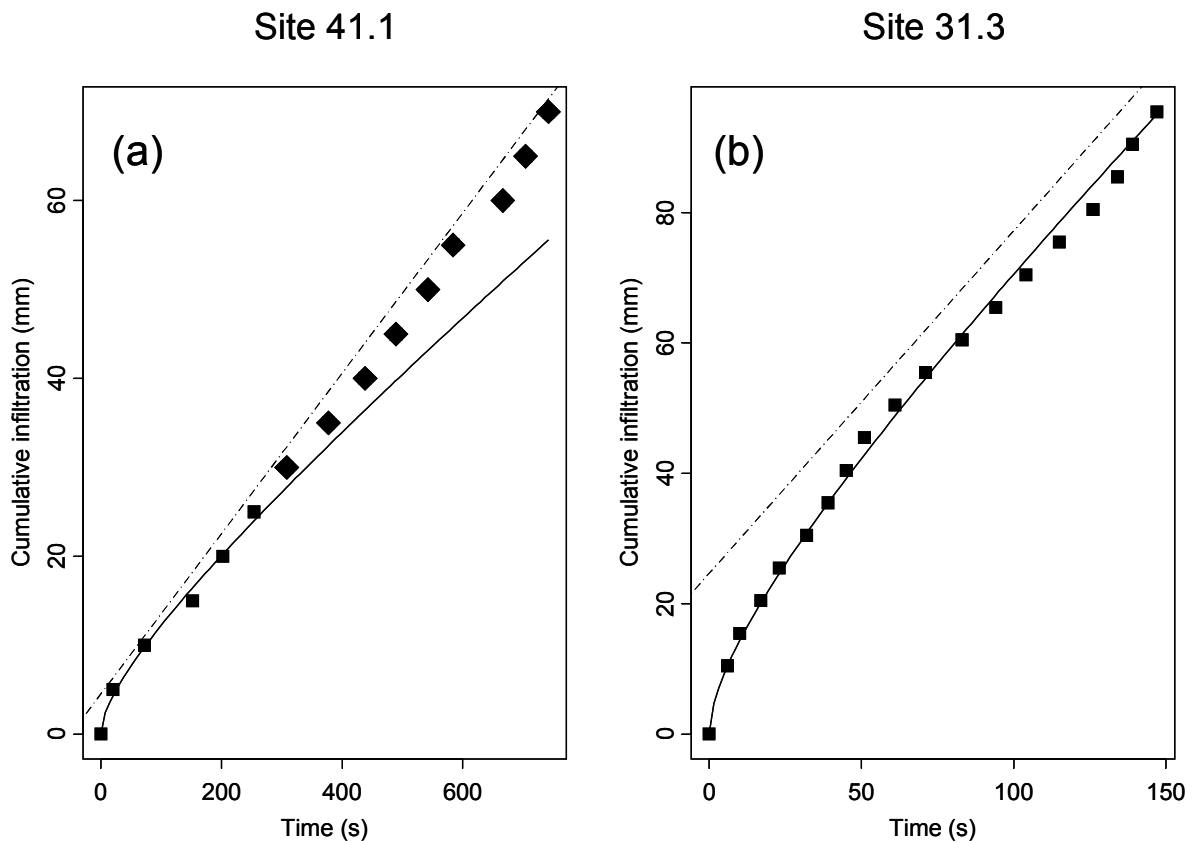
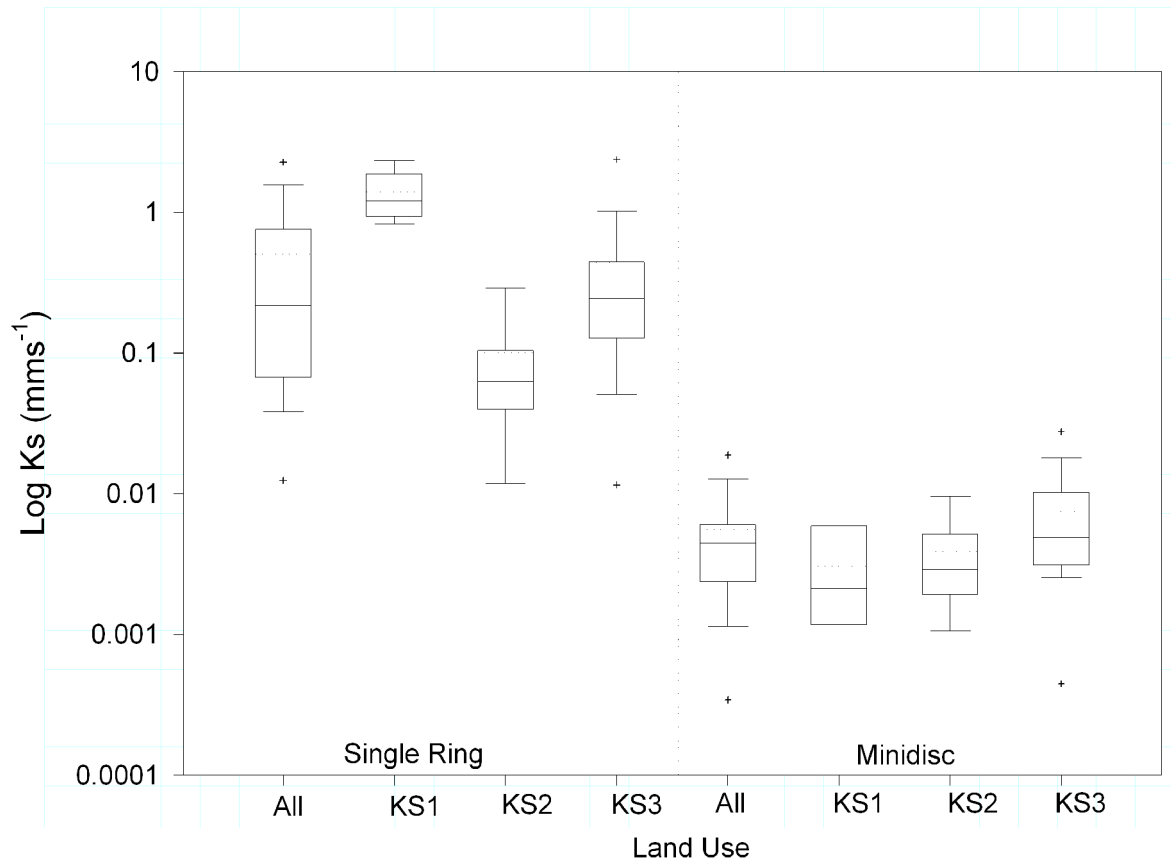


Figure 6. Observed (points) and fitted cumulative infiltration data for sites 41.1 (Open space in forest) and 31-3 (orchards). The full line is the fit of Eq. (6) for short time steps and the dashed line is the fit of Eq. (10) for large time steps. Eq. (6) was fitted to the points plotted with squares.

1



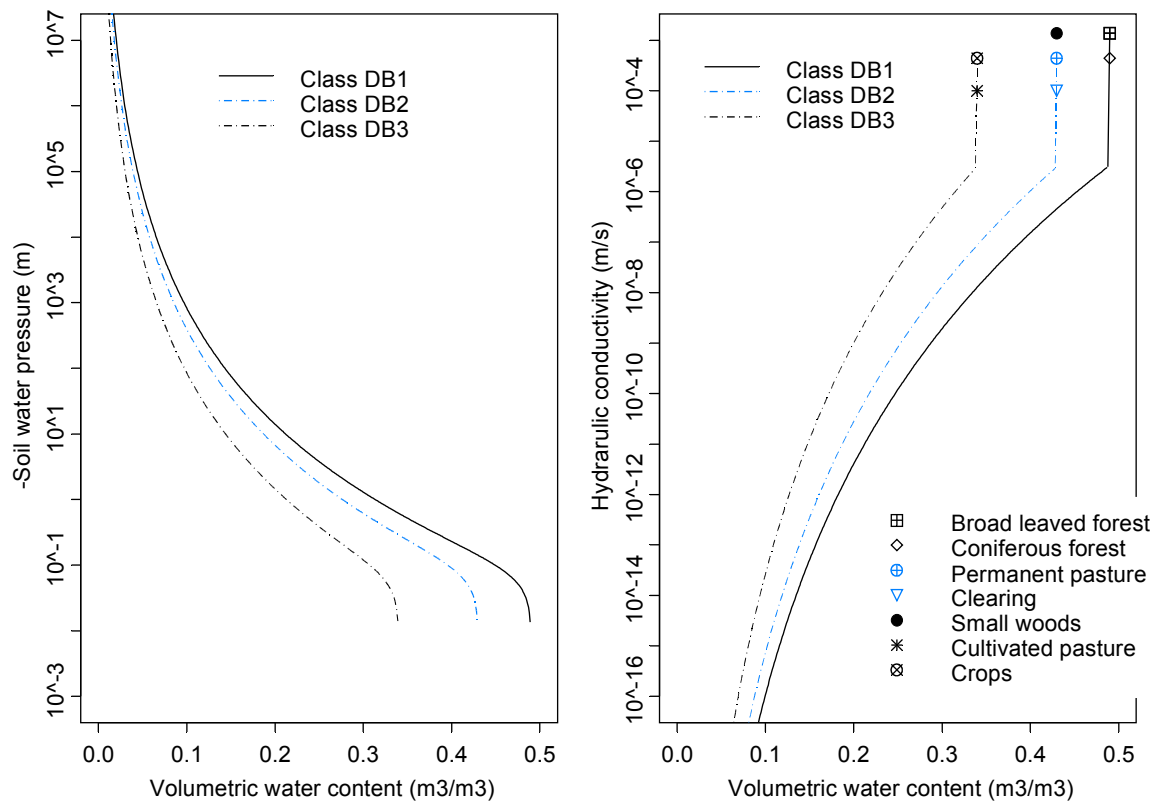
1

2 Figure 7. Box plots of saturated hydraulic conductivity (single ring) and hydraulic
3 conductivity at -20 mm (mini-disk) for all the samples and the three identified classes
4 KS1, KS2 and KS3.

5

1

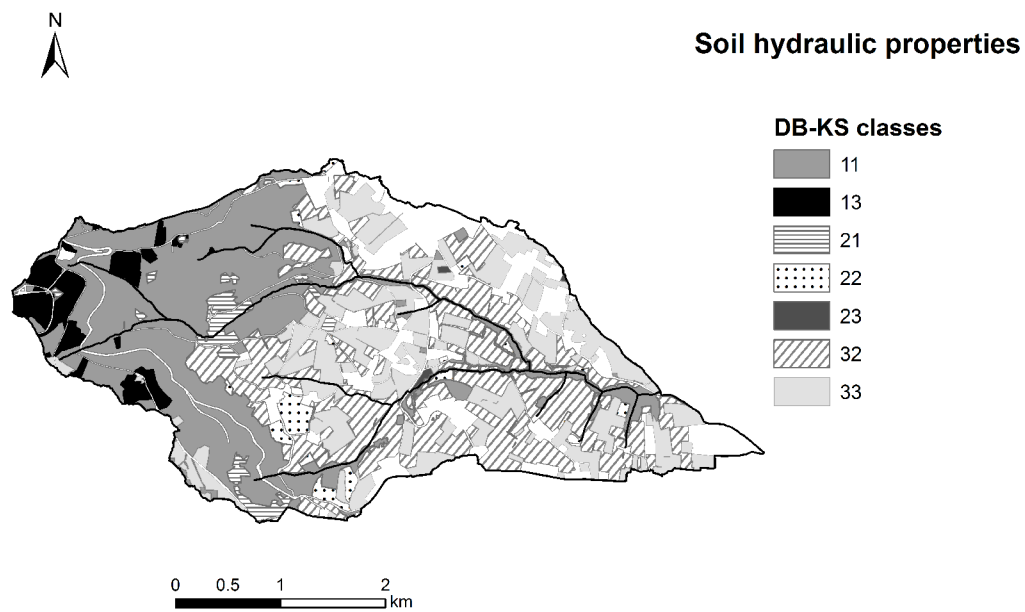
1



2

Figure 8. Estimated retention curves and hydraulic conductivity curves for the combination of classes DB1, DB2, DB3. Between near-saturated and saturated hydraulic conductivity, a linear relationship on the natural logarithm of hydraulic conductivity versus soil water content was assumed. The symbols are the saturated hydraulic conductivities for the various combinations of DB and KS classes: broad leaved forest (DB1-KS1); coniferous forest (DB1-KS3); permanent pasture (DB2-KS3); clearing (DB2-KS2); small woods (DB2-KS1); cultivated pasture (DB3-KS2); crops (DB3-KS3)..

1



1

2Figure 9. Mapping of soil hydraulic properties. The classes numbering is provided in Table
3VII. White surfaces correspond to the non sampled areas defined in Table VII.